(12)

AD F300 297

AD A130874

MEMORANDUM REPORT ARBRL-MR-03285

(Supersedes IMR No. 757)

# INSTABILITIES OF A GYROSCOPE PRODUCED BY RAPIDLY ROTATING, HIGHLY VISCOUS LIQUIDS

William P. D'Amico, Jr.



June 1983

US ARMY ARMAMENT RESEARCH AND DEVELOPMENT COMMAND
BALLISTIC RESEARCH LABORATORY
ABERDEEN PROVING GROUND, MARYLAND

Destroy this report when it is no longer needed.
Do not return it to the originator.

Additional copies of this report may be obtained from the National Technical Information Service, U. S. Department of Commerce, Springfield, Virginia 22161.

The findings in this report are not to be construed as an official Department of the Army position, unless so designated by other authorized documents.

The use of trade names or manufacturers' names in this report does not constitute indorsement of any commercial product.

UNCLASSIFIED

SECURITY CLASSIFICATION OF THIS PAGE (When Data Entered)

| REPORT DOCUMENTATION PAGE | READ INSTRUCTIONS BEFORE COMPLETING FORM |
|---|---|
| 1. REPORT NUMBER: MEMORANDUM REPORT ARBRL-MR-03285 | 2. GOVT ACCESSION NO.: AD-A130 874 |
| 3. RECIPIENT'S CATALOG NUMBER | |
| 4. TITLE (and Subtitle): INSTABILITIES OF A GYROSCOPE PRODUCED BY RAPIDLY ROTATING, HIGHLY VISCOUS LIQUIDS | 5. TYPE OF REPORT & PERIOD COVERED: Final |
| | 6. PERFORMING ORG. REPORT NUMBER |
| 7. AUTHOR(s): William P. D'Amico, Jr. | 8. CONTRACT OR GRANT NUMBER(s) |
| 9. PERFORMING ORGANIZATION NAME AND ADDRESS: US Army Ballistic Research Laboratory<br>ATTN: DRDAR-BLL<br>Aberdeen Proving Ground, MD 21005 | 10. PROGRAM ELEMENT, PROJECT, TASK AREA & WORK UNIT NUMBERS: RDT&E 1L162618AH80 |
| 11. CONTROLLING OFFICE NAME AND ADDRESS: US Army Armament Research & Development Command<br>US Army Ballistic Research Laboratory (DRDAR-BLA-S)<br>Aberdeen Proving Ground, MD 21005 | 12. REPORT DATE: June 1983<br>13. NUMBER OF PAGES: 56 |
| 14. MONITORING AGENCY NAME & ADDRESS (if different from Controlling Office) | 15. SECURITY CLASS. (of this report): Unclassified<br>15a. DECLASSIFICATION/DOWNGRADING SCHEDULE |

16. DISTRIBUTION STATEMENT (of this Report)

Approved for public release; distribution unlimited.

17. DISTRIBUTION STATEMENT (of the abstract entered in Block 20, if different from Report)

18. SUPPLEMENTARY NOTES

This report supersedes IMR 757 dated November 1982.

19. KEY WORDS (Continue on reverse side if necessary and identify by block number)

Rotating Liquids
Low Reynolds Number
Yaw Moment

20. ABSTRACT (Continue on reverse side if necessary and identify by block number) (lcb/bja)

A series of experiments were conducted to determine the yaw behavior of a gyroscope that contained a liquid-filled rotor. Spin rates, liquid viscosities, and cylinder geometries were selected to produce a wide range of Reynolds numbers ($5 < Re < 12{,}000$). Three cylinder aspect ratios (height/diameter) were tested: 1/1, 3/2, and 3/1. Coning frequencies for the free gyroscope were selected to be typical of spin-stabilized projectiles. Two distinct types of yaw behavior were observed with Reynolds number being the major controlling

(Continued)

DD FORM 1 JAN 73 1473 EDITION OF 1 NOV 65 IS OBSOLETE

UNCLASSIFIED

SECURITY CLASSIFICATION OF THIS PAGE (When Data Entered)

20. ABSTRACT (Continued):

parameter. For Re > 1,000, the motion of the gyroscope was reasonably well predicted by classical liquid-filled shell theories that postulate a resonance between a natural frequency of the spinning liquid and the yaw frequency of the gyroscope. For these conditions the maximum yaw growth rate will occur when an eigenfrequency of the liquid is approximately equal to the gyroscope yaw frequency. For cases where Re < 1,000, the behavior of the gyroscope was not characterized by a resonant mechanism. Instead, the liquid-induced yaw moments and yaw growth rates grew monotonically with increasing yaw frequencies.

TABLE OF CONTENTS

## LIST OF ILLUSTRATIONS

LIST OF ILLUSTRATIONS (Continued)

LIST OF ILLUSTRATIONS (Continued)

# I. INTRODUCTION

A substantial amount of research has been conducted on the stability of the motion of spinning, liquid-filled containers. Areas of interest can be quite diverse. Two such examples are: the geophysical problem of the motion of the fluid core of the earth or the flight stability of a spin-stabilized liquid payload artillery projectile. Most experience in rotating liquid flows is for cases where the rotational force is much larger than the viscous force, i.e., high Reynolds number (Re) flows.* This paper deals with a series of experiments that were conducted for $5 < Re < 12{,}000$. This range of Re has previously not been examined.

Stewartson treated the stability of the motion of a liquid-filled top.[1] In this analysis, the inviscid liquid was assumed to be spinning as a quasi-rigid body with the angular velocity of the top. It was determined that the yawing motion of the top could excite the natural frequencies of oscillation of the liquid (the eigenfrequencies) and a moment due to the pressure disturbances within the liquid could destabilize the motion of the top. Wedemeyer[2] incorporated viscosity into the Stewartson theory through the use of boundary layer type corrections, and the Stewartson-Wedemeyer theory has compared favorably with gyroscope experiments conducted by Karpov.[3] Recent analyses by Murphy[4] and by Gerber, et al,[5] represent more complete and rigorous models than the Stewartson-Wedemeyer theory, but all of these treatments are still limited to "high Reynolds numbers" due to viscous corrections at the walls of the container.

---

* *Reynolds number is defined as $a^2\dot{\phi}/\nu$ (where a is the radius of a cylindrical cavity, $\dot{\phi}$ is the spin, and $\nu$ is the kinematic viscosity of the liquid) and is physically the ratio of the rotational force to the viscous force. This definition is simply the inverse of the Ekman number which is typically used in analyses of rotating liquid flows.*

1. *K. Stewartson, "On the Stability of a Spinning Top Containing Liquid," Journal of Fluid Mechanics, Vol. 5, 1959, pp. 577-592.*

2. *E. H. Wedemeyer, "Viscous Corrections to Stewartson's Stability Criterion," BRL Report No. 1325, June 1966 (AD 489687).*

3. *B. G. Karpov, "Liquid-Filled Gyroscope: The Effect of Reynolds Number on Resonance," BRL Report No. 1302, October 1965 (AD 479430).*

4. *Charles H. Murphy, "Angular Motion of a Spinning Projectile With a Viscous Liquid Payload," BRL Memorandum Report No. ARBRL-MR-03194, August 1982 (AD A118676).*

5. *Nathan Gerber and Raymond Sedney, "Moment on a Liquid-Filled Spinning and Nutating Projectile: Solid Body Rotation," BRL Technical Report No. ARBRL-TR-02470 (AD A125332).*

For low Reynolds number rotating flows, D'Amico and Miller observed large yaw and despin moments.[6] Miller conducted laboratory experiments using a fixed precession angle spin fixture and determined despin moments over a wide range of Reynolds number (Figure 1).[7] The maximum despin moment is at Re = 10. D'Amico fired yawsonde-instrumented projectiles which produced rapid yaw growth and violent despin histories for approximately that same Reynolds number.[8,9] This report describes a series of laboratory experiments where the liquid-induced yaw moment was measured as a function of the yawing frequency of a gyroscope. The spin of the gyroscope was held constant (no despin moments will be reported), and the yawing motion of the gyroscope was less than 5 degrees. The Reynolds number range for these data are $5 < Re < 12{,}000$. Comparisons of liquid-induced yaw moment coefficients for flight and gyroscope tests are made. Correlations for the liquid-induced yaw moment with pertinent dimensionless groups are made. Also, a lower bounds in Reynolds number was tentatively established for the application of viscous corrected theories such as Murphy[4] and Gerber, et al.[5]

## II. LABORATORY GYROSCOPE

### A. Simulation of a Spin-Stabilized Projectile With a Gyroscope

A freely gimballed gyroscope similar to that used by Karpov[3] was used to measured the yaw moments produced by a highly viscous, rotating liquid. A short explanation of the dynamical behavior of the gyroscope will aid in the interpretation of the test data and results. A spin-stabilized projectile experiences a complicated angular motion during free-flight. Only certain aspects of this free-flight motion will be simulated by the gyroscope. Murphy has analyzed the motion of a spin-stabilized projectile[10] For the case of a projectile which does not contain a liquid and where the effects of drag are neglected, the angular motion is described by

---

6. *V. P. D'Amico and M. C. Miller, "Flight Instability Produced by a Rapidly Spinning, Highly Viscous Liquid," Journal of Spacecraft and Rockets, Vol. 16, No. 1, January-February 1979, pp. 62-64.*

7. *Miles C. Miller, "Flight Instabilities of Spinning Projectiles Having Non-Rigid Payloads," Journal of Guidance Control and Dynamics, Vol. 5, March-April 1982, pp. 151-157.*

8. *V. P. D'Amico, W. H. Clay, and A. Mark, "Diagnostic Tests for Wick-Type Payloads and High Viscosity Liquids," BRL Memorandum Report No. ARBRL-MR-02913, April 1979 (AD A072812).*

9. *V. P. D'Amico and W. H. Clay, "High Viscosity Liquid Payload Yawsonde Data for Small Launch Yaws," BRL Memorandum Report No. ARBRL-MR-03029, June 1980 (AD A088411).*

10. *Charles H. Murphy, "Free Flight Motion of Symmetric Missiles," BRL Report No. 1216, July 1963 (AD 442757).*

$$\ddot{\tilde{\xi}} + (\hat{H} - i\sigma\dot{\phi})\,\dot{\tilde{\xi}} - (\hat{M} + i\sigma\dot{\phi}\hat{T})\,\tilde{\xi} = 0 \tag{1}$$

where $\tilde{\xi}$ is the complex yaw within a nonrolling coordinate system and

$\hat{H}$ = damping moment = $(\rho S\ell/2m)\left[C_{N_\alpha} - k_y^{-2}\left(C_{M_q} + C_{M_{\dot{\alpha}}}\right)\right]$

$\hat{M}$ = static moment = $(\rho S\ell^3/2I_y)\;\; C_{M_\alpha}\,(V/\ell)^2$

$\hat{T}$ = Magnus moment = $(\rho S\ell/2m)\;\left[C_{N_\alpha} + k_x^{-2}\,C_{M_{p_\alpha}}\right]\;(V/\ell)$

$\dot{\phi}$ = spin rate

$\sigma = I_x/I_y$

If an epicyclic motion is assumed for the empty projectile, then

$$\tilde{\xi} = K_1 e^{i\phi_1} + K_2 e^{i\phi_2} \tag{2}$$

where ordinarily

$$K_j = K_j\, e^{\epsilon_j \dot{\phi}_j t}\,, \qquad j = 1,\ 2 \tag{3}$$

$$\dot{\phi}_j = \dot{\phi}_{jo} + \tau_j \dot{\phi}_j t \tag{4}$$

$$\tau_j = (\sigma/2)\,(1 \pm \sqrt{1 - 1/s_g}) \tag{5}$$

where $s_g$ is the gyroscopic stability factor, $I_x$ and $I_y$ are the axial and transverse moments of inertia, and $\tau_1$ and $\tau_2$ are the fast and slow yaw frequencies. (A spin stabilized projectile has two modes of precession or yaw.) Explicit forms for the yaw growth rate ($\epsilon_j$) and the gyroscopic stability factor are

$$\epsilon_j = - (\tau_j \hat{H} - \sigma \hat{T})/[(2\tau_j - \sigma)\ (\tau_j \dot{\phi})] \tag{6}$$

$$s_g = \sigma^2\ \dot{\phi}^2/4\hat{M} \tag{7}$$

A gyroscope has a gravity moment ($\hat{G}$) that acts in a similar fashion as the static moment $\hat{M}$. Experience with the gyroscope has shown that both precessional modes will damp when the center of mass is slightly below the gimbal pivots. For this configuration $\hat{G} < 0$. The direction of $\dot{\phi}_1$ will be the same as $\dot{\phi}$, while the direction of $\dot{\phi}_2$ will be opposite to $\dot{\phi}$. The gyroscope stability factor will be negative since $\hat{G} < 0$. However, $|s_g| >> 1$ and for the empty gyroscope,

$$\tau_1 \equiv \sigma \qquad \text{and} \qquad \tau_2 \equiv 0 \tag{8}$$

Typically, the gyroscope is operated such that $0.04 < \tau_1 < 0.10$ and $|\tau_2| < 0.005$, which corresponds to the conditions set out in Equation (8).

A form for the liquid moment has also been suggested by Murphy.[4]

$$M_{LY} + i\ M_{LZ} = m_L\ a^2 \dot{\phi}^2 \left[ \tau_1\ C_{LM_1}\ K_1\ e^{i\phi_1} + \tau_2\ C_{LM_2}\ K_2\ e^{i\phi_2} \right], \tag{9}$$

where the liquid moment was scaled by the liquid mass ($m_L$), cylinder radius ($a$), and the spin ($\dot{\phi}$). This internal liquid moment can be incorporated into the projectile description provided by Eq. (1),

$$\ddot{\tilde{\xi}} + (\hat{H} - i\sigma\dot{\phi})\ \dot{\tilde{\xi}} - (\hat{M} + i\sigma\dot{\phi}\ \hat{T})\ \tilde{\xi} =$$

$$i\ \dot{\phi}^2\ (m_L a^2/I_y) \left[ \tau_1\ C_{LM_1}\ K_1 e^{i\phi_1} + \tau_2\ C_{LM_2}\ K_2\ e_2^{i\phi_2} \right] \tag{10}$$

Several assumptions valid for the gyroscope can be made to simplify this equation. First, damping rates for the empty gyroscope are very small (typically $\varepsilon_j \leq -5 \times 10^{-3}$). Hence, the only moment acting on the gyroscope will be that produced by the liquid. Second, the yawing motion will be assumed to consist of only the fast yaw mode; i.e., $\tilde{\xi} = K_1 e^{i\phi_1}$. Third, $C_{LM}$ will ultimately depend upon many variables ($K_1$, $\tau_1$, $\varepsilon_1$, Re, c/a), but a simple form from Reference 4 will be used when the spin is positive.

$$C_{LM_j} = C_{LSM_j} + i\, C_{LIM_j} \tag{11}$$

$C_{LSM}$ is a side moment coefficient that controls the projectile system yaw damping, while $C_{LIM}$ is an in-plane moment coefficient that principally modifies the frequency of motion.

General expressions for yaw frequencies and yaw growth (or damping) rates can be obtained from Equations (10) and (11):

$$\tau_j = (\sigma/2)\left[f_j - (-1)^j \sqrt{f_j^2 - (1/s_g)}\,\right] \tag{12}$$

for

$$f_j = 1 + (m_L\, a^2/I_x)\, C_{LIM_j}$$

and

$$\varepsilon_j = (m_L a^2/I_x)\,(2\tau_j/\sigma - 1)^{-1}\, C_{LSM_j} \tag{13}$$

Equations (12) and (13) can be inverted to obtain expressions for $C_{LIM_j}$ and $C_{LSM_j}$ based upon experimentally determined values of $\varepsilon_j$ and $\tau_j$. During the course of the experiments it was observed that $\tau$ for the liquid-filled gyroscope was within 1% of $\tau$ for the empty gyroscope. This small difference is the effect of $C_{LIM}$ on $\tau$. Attempts were made to utilize this small difference between the liquid-filled and empty coning frequencies to establish $C_{LIM}$ values. It was found that the frequency measurements were not sufficiently

accurate to predict $C_{LIM}$. Equation (13) will be used to determine $C_{LSM}$. The stability of the gyroscope is controlled by the liquid, and the motion is dominated by the fast yaw mode. The yawing motion is essentially a single mode coning motion. As such, the dimensionless fast yawing frequency will be referred to as the coning frequency, i.e., $\tau = \tau_1$, and the yaw growth rate of the fast mode is redefined as $\epsilon_1 = \epsilon$. For $\tau = \sigma$ and $\hat{H} = \hat{T} = 0$, then, Equation (13) becomes

$$C_{LSM} = \epsilon/(m_L a^2/I_x) \ . \tag{14}$$

The above formulation also assumes that $\epsilon$ is relatively small. For the experimental data presented here, $\epsilon < 0.02$, and Equation (14) can be used.

B. Operation of a Liquid-Filled Gyroscope

Cylindrical containers are located within the rotor of a freely gimballed gyroscope (Fig. 2). The inner gimbal supports the rotor and the test cylinders. Weights can be located on the rotor to control $I_x$. Weights can also be attached to the top or bottom of the inner gimbal. During the course of a test run, a DC motor (located beneath the inner gimbal) drives the rotor at a constant rate. The positions of the weights located on the inner gimbal can be moved to vary $I_y$, and these weights are used to control $I_x/I_y$, which from Eq. (8) provides control of the coning frequency. The center of gravity of the rotor/inner gimbal is selected to be slightly below the support pivots. The pivots consist of crossed spring leaves (so called flexural pivots) instrumented with strain gages. With the aid of usual bridge circuit techniques, strain is calibrated as a function of deflection. The response of the measurement system is linear for deflections up to ten degrees.

The yaw of the gyroscope is the angle between the vertical and the spin axis of the rotor. The liquid is allowed ample time to achieve a state of rigid body rotation prior to the rotor being released. The inner gimbal is released from the vertical position without any initial disturbance. Unstable motion, if it occurs, is normally self starting from the vertical position. The yawing histories for each set of experiments are digitized and passed to a computer. The computer processes the yaw record to determine a $K_1$ history. An initial amplitude is determined, $K_{10}$, and is used as a reference by which all successive $K_1$ values are scaled. The ratio $[\ln (K_1/K_{10})]$ is displayed versus the time. A sample reduction for $\ln (K_1/K_{10})$ versus time is shown in Figure 3. A linear variation of $\ln (K_1/K_{10})$ indicates a constant growth rate for exponential variations in $K_1$. The data are fit by a linear least squares technique to determine the growth rate. Three cylinders were tested. Height (2c), diameter (2a), aspect ratio (c/a), and offset (h) of the geometric center of the cylinder from the gimbal pivots are listed below:

| Cylinder Type | Height (cm) | Diameter (cm) | c/a | Offset (cm) |
|---|---|---|---|---|
| 1/1 | 13.246 | 12.718 | 1.042 | -1.530 |
| 3/2 | 18.854 | 12.690 | 1.486 | +5.887 |
| 3/1 | 25.768 | 8.242 | 3.126 | -0.959 |

The cylinders are referenced by their approximate aspect ratio which corresponds to the cylinder type as listed above. Silicon oils were used as test fluids. The kinematic properties of these oils are given below.

| Viscosity Ratio ($\nu/\nu_{water}$) | Kinematic Viscosity (cs) | Density (gm/cc) |
|---|---|---|
| 100 | 102.4 | 0.972 |
| 500 | 528.6 | 0.972 |
| 1,000 | 1,004.5 | 0.974 |
| 10,000 | 9,468.5 | 0.953 |
| 60,000 | 58,955 | 0.960 |
| 100,000 | 101,772 | 0.963 |

Water has a kinematic viscosity of approximately 1 cs = 0.01 $cm^2/s$ under standard conditions. Most of the data were taken at a spin rate of 50 Hz; however, some data trials were made at 33.3 Hz, 41.6 Hz, or 58.3 Hz. For a particular cylinder, viscosity, and spin, the stability of the gyroscope was measured over a wide range of coning frequencies. For the higher viscosity oils, a rapid survey at three coning frequencies was used, while for the lower viscosity oils, a dense survey of coning frequencies was made to produce a detailed response curve. In summary, the parameters that were varied during the experiments were: cylinder aspect ratio (c/a), kinematic viscosity ($\nu$), spin rate ($\dot{\phi}$), and coning frequency ($\tau$). Control of these parameters produced the following ranges: $5 \leq Re \leq 12{,}000$ and $0.04 < \tau < 0.1$.

## III. LIQUID-FILLED GYROSCOPE EXPERIMENTS

Two objectives were outlined for the gyroscope tests: (1) Determine the yaw moments produced for low Reynolds numbers and (2) Determine the validity of linear models that utilize boundary-layer corrections (References 4 and 5) as a function of Reynolds number. The liquid moment will have a complicated behavior, but the primary independent variables are Re, c/a, $\tau$, $K_1$, and $\varepsilon$. Previously during experimental investigations of high Re rotating flows, nonlinear or nonstationary behavior has been observed as a function of

$K_1$.[11,12] In the present experiments for Re < 12,000, such nonlinear or nonstationary behavior was not observed for $K_1$ < 5 deg; i.e., for exponential behavior, constant growth rates were observed. The basic measurement of a yaw growth rate will normally be converted into $C_{LSM}$. The use of $C_{LSM}$ will also allow for the comparison of the gyroscope data with existing flight data. $C_{LSM}$ is usually presented as a function of the coning frequency ($\tau$) or the product Re $\cdot$ $\tau$, which is a Reynolds number whose characteristic frequency is based upon the fast yaw frequency ($\dot{\phi}_1$) rather than the spin rate ($\dot{\phi}$).

An estimation of experimental errors for the gyroscope data was not specifically performed. Rather, multiple runs for the same set of test conditions were recorded and analyzed. All of these runs are provided, thus indicating the repeatability of the entire measurement and data reduction procedure.

The wide range in Reynolds number is primarily achieved by the choice of the viscosity of the liquid. For Re > 5,000, the aspect ratios of the 1/1 and 3/1 cylinders were selected such that $\tau$ was sufficiently close to an eigenfrequency to produce unstable yawing motion. (The aspect ratio of the 3/2 cylinder was specifically chosen not to be close to an eigenfrequency and, therefore, would have a stable yawing motion for large Re.) Comparisons between experimental data and models that use boundary-layer viscous-type corrections should be good for "large" Reynolds numbers. Figure 4a provides such a comparison for the 1/1 cylinder when Re = 12,400. Within Reference 4, growth rate predictions were made for incremental changes in c/a. A slightly better correlation with the experimental data was obtained when the computational aspect ratio was increased by 0.5%. Figure 4a does not include predictions of growth rate for slightly modified c/a values. Figures 4b and 4c show comparisons of theory and experiment for c/a = 1/1 for Re = 2,400 and Re = 1,260. It is not clear whether the differences between the observed and predicted growth rates are due to small measurement errors in c/a or increased viscous forces. However, the agreement is still sufficiently good for practical applications. Figures 5a and 5b present comparisons for the 3/1 cylinder when Re = 5,210 and Re = 1,010. The agreement between experiment and theory is not good. Within Reference 4, comparisons of theory and experiment were substantially better for Re = 9,000 and Re = 520,000. All of the data in Figures 4-5 have a similar character: nonmonotonic dependence of growth rate with coning frequency. For Re < 1,000, the nature of the response curve (for the same range in coning frequency) changes dramatically. Experimental data for these cases will be presented in the form of a liquid side moment coefficient ($C_{LSM}$) rather than growth rate to allow a comparison with flight data.

---

11. *W.E. Scott and W.P. D'Amico, "Amplitude-Dependent Behavior of a Liquid-Filled Gyroscope," Journal of Fluid Mechanics, Vol. 60, Part 4, 1973, pp. 751-758.*

12. *Richard D. Whiting, "An Experimental Study of Forced Asymmetric Oscillations in a Rotating Liquid-Filled Cylinder," BRL Technical Report No. ARBRL-TR-02376, October 1981 (AD A107948).*

A. Data for a Viscosity Ratio of 10,000

Figures 6a-c give $C_{LSM}$ versus $\tau$ for a viscosity ratio of 10,000. It is seen that $C_{LSM}$ is nearly linear with $\tau$ for all cases. Small changes in Re were obtained by different spin rates. Changes in $C_{LSM}$ that were produced by variations in spin can be correlated by using Re $\cdot$ $\tau$ rather than simply $\tau$, as seen in Figures 6d-f. However, $C_{LSM}$ data for different aspect ratios (but identical spin rates) are not well correlated by Re $\cdot$ $\tau$.

B. Data for a Viscosity Ratio of 60,000

Figures 7a-c show $C_{LSM}$ versus $\tau$ for a viscosity ratio of 60,000. As before, it is observed that $C_{LSM}$ is linear with $\tau$ and that small variations in spin can be correlated by using Re $\cdot$ $\tau$ (Figures 7d-f). However, in some cases for lower spin and/or coning frequencies, the gyroscope was stable. Figure 7g also shows that data from different aspect ratios are not well correlated by Re $\cdot$ $\tau$.

C. Data for a Viscosity Ratio of 100,000

Figure 8 gives data for a viscosity ratio of 100,000. Very little data were taken since the gyroscope was often stable. A linear variation of $C_{LSM}$ with $\tau$ is observed.

D. Correlation of Data for Viscosity Ratios of 10,000, 60,000 and 100,000

A large volume of data now exists for low Re where $C_{LSM}$ varies linearly with $\tau$. All of the data are shown in Figure 9 with Re $\cdot$ $\tau$ as the correlation parameter. From previous plots, it was expected that a good correlation would not occur. However, the expanded scale artificially enhanced the correlation, except now the data are clustered based upon the viscosity ratio of the test liquid; i.e., all the data for Re $\cdot$ $\tau > 4$ are for a viscosity ratio of 10,000. The $C_{LSM}$ data were plotted against combinations of (Re, $\tau$, c/a). A correlation for $C_{LSM} = 0.0125 + 0.0756\ (Re)(\tau^2)(c/a)^{-1}$ was selected by a linear least squares fit and is presented in Figure 10. Several deficiencies are obvious. First, much of the data for very low Re are collapsed near the origin. However, the larger (and potentially destabilizing) values of $C_{LSM}$ are well correlated.

E. Comparison With Flight Data

Flight data from projectiles are available within References 8 and 9. Unfortunately, flight data and gyroscope data are not at the same aspect ratio and Reynolds number, although new tests are planned to match flight and gyroscope conditions. Yawsonde data were processed for $C_{LSM}$ in a fashion similar to that of the gyroscope data. The amplitude of the yaw was greater than that of the gyroscope. The effects of aerodynamic damping were neglected, but the flight Mach numbers were transonic and under such conditions the aerodynamic

damping of the projectile is small. Figure 11 shows a comparison between flight data (Reference 9, Round E1-9542) and gyroscope data for comparable Reynolds numbers. Figure 12 shows a second comparison between flight data (Reference 8, Round E1-9396) and gyroscope data. Due to the differences in both Re and c/a, comparisons may not be valid. However, the flight and gyroscope determined $C_{LSM}$ data are similar in both cases. The data in Figure 11 show a consistent trend in $\tau$, but this did not occur in Figure 12. A data comparison for a wide range of $\tau$ would be difficult, since projectiles normally have $\tau \sim 0.08$. The flight data can also be compared with the correlation suggested in Figure 10. For Re = 13.1 and $C_{LSM} = 0.0153$, $(Re)(\tau)(c/a)^{-1} = 0.024$, while for Re = 336 and $C_{LSM} = 0.020$, $(Re)(\tau)(c/a)^{-1} = 0.76$. The Re = 13.1 datum falls close to the suggested correlation, but the Re = 336 datum does not agree with the correlation. The poor correlation of the Re = 336 datum could be attributed to the differences seen in Figure 12 for the simple comparison of $C_{LSM}$ versus $\tau$.

## IV. DISCUSSION

Yaw moments from the gyroscope can be readily displayed as simple functions of the Reynolds number. For data sets where c/a, $\nu$, and $\dot{\phi}$, are constants, $C_{LSM}$ can be averaged over $\tau$ or

$$C_{LSM_{ave}} = f\ (c/a,\ Re)\ .$$

Figures 13a-c show $C_{LSM_{ave}}$ versus Reynolds number. The scales of these figures are identical to emphasize various aspects of the data. In Figure 13a, $C_{LSM_{ave}}$ dramatically increases as the Reynolds number increases. $C_{LSM_{ave}}$ does not decrease for extremely high Re values (as did the despin moment data in Figure 1). The resonance between the coning frequency and the liquid eigenfrequency for c/a = 1/1 only becomes stronger as Re increases. A similar situation exists for c/a = 3/1. However, the effects are much less obvious, as seen in Figure 13b. The resonance with the liquid eigenfrequency is much weaker for c/a = 3/1 than for c/a = 1/1. The 3/2 cylinder was specifically chosen so as not to produce a resonance within the range of experimentally produced coning frequencies. The yaw behavior for c/a = 3/2 indicates a maximum $C_{LSM_{ave}}$ for Re < 100, with smaller yaw moments for either larger or smaller Reynolds numbers (as in Figure 13c). This type of behavior is similar in character to the despin moment data.

A typical response curve for large Reynolds numbers is shown in Figure 4a. Response curves for lower Reynolds numbers show substantially reduced growth rates (Figures 4b and 4c). The predicted growth rates increase linearly with $\tau$ until the maximum growth rate is achieved. Also note from Figures 14a-c, that as the Reynolds number was reduced, the coning frequency for maximum growth rate increased. For Re < 1,000, the maximum growth rate may

shift to $\tau > 0.1$. Thus, growth rates would increase linearly with coning frequency for $\tau < 0.1$. This is exactly what is observed. A continued reduction in Re will eventually give extremely large viscous damping and unstable yaw behavior will not be possible.

The previous rationale is not applicable to the 3/2 cylinder. Murphy[4] has shown that the average value of the liquid moment is increased by a reduction in Re. Hence, for a nonresonant cylinder, such as c/a = 3/2, large Re behavior is stable while low Re behavior could be unstable. When Re approaches unity, however, the liquid will act as a rigid body and no destabilizing effects will be observed. This mechanism is in qualitative agreement with the data for the 3/2 cylinder as shown in Figure 13c.

## V. SUMMARY

Comparisons between gyroscope data and theory were consistent for c/a = 1/1 for Reynolds numbers as small as 1,010, but comparisons were inconsistent for c/a = 3/1 when Re = 5,210. This indicates that theoretical models with viscous corrections of order $Re^{-1/2}$ may have a Reynolds number and aspect ratio limit when the Reynolds number approaches 1,000. Yaw moments for highly viscous flows are probably not generated from a new mechanism, but rather are the remnants of high Reynolds number resonances. However, the liquid-induced yaw moments are sufficiently large for $10 < Re < 100$ to destabilize the yawing motion of a spinning projectile or a gyroscope.

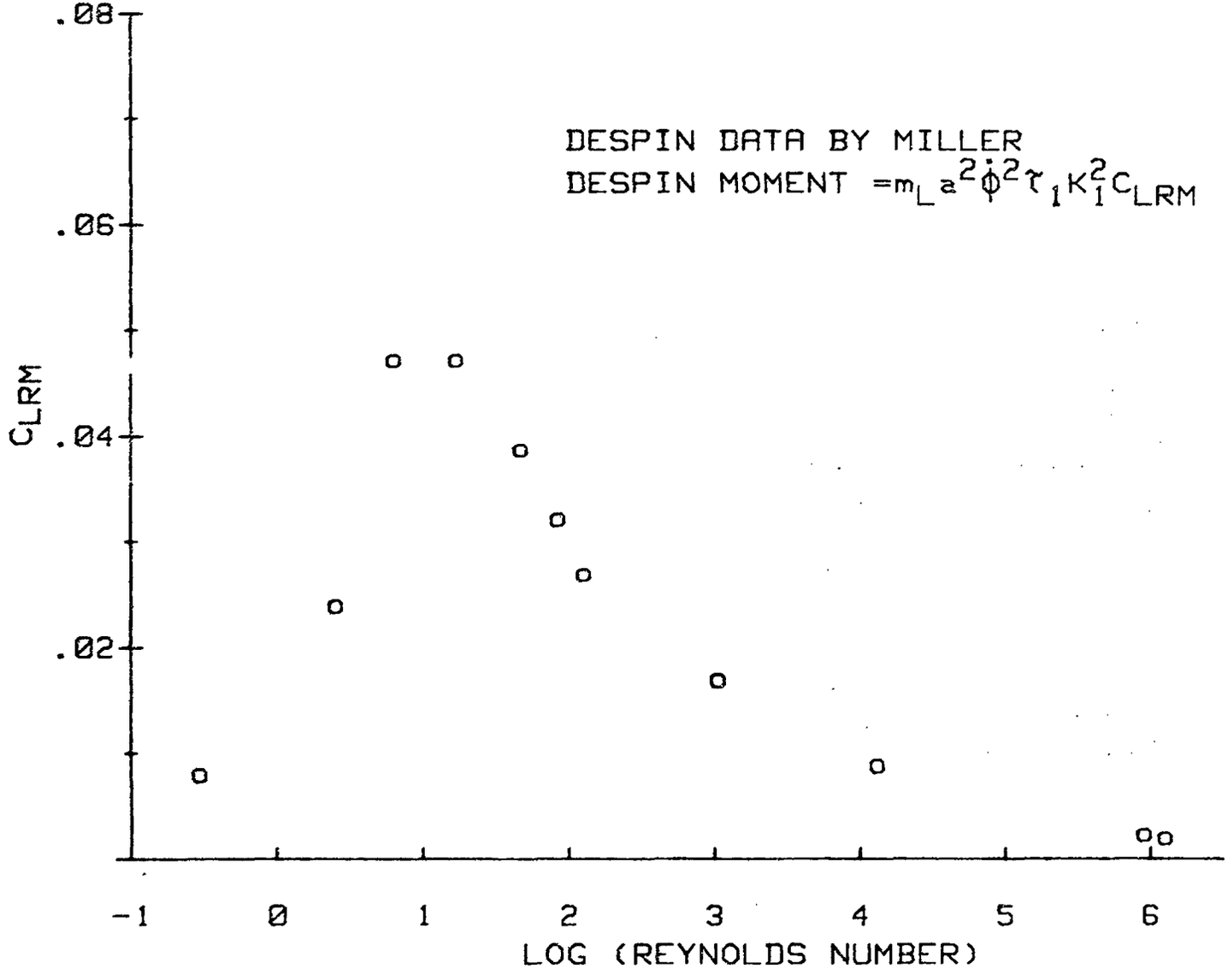


Figure 1. Despin Moment Data by Miller (Ref. 6)

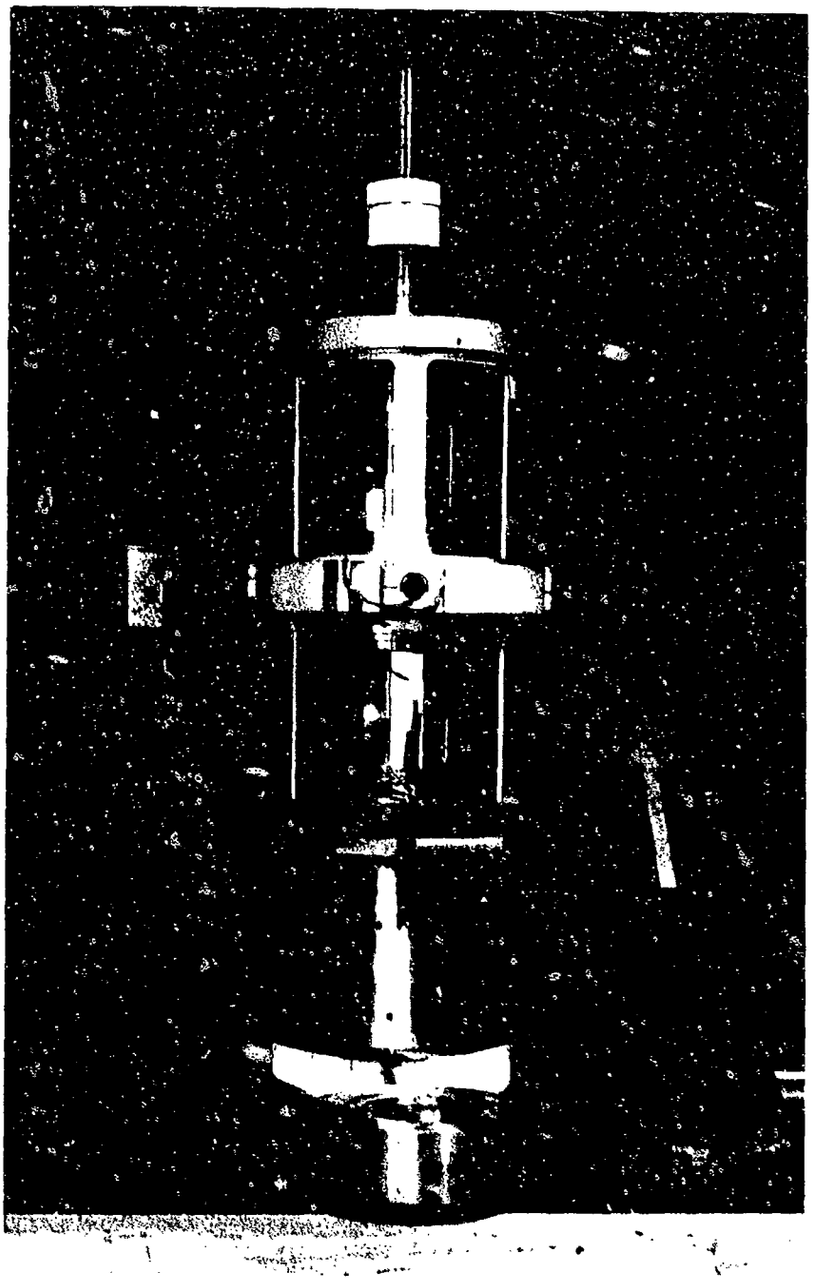

Figure 2. Laboratory Gyroscope

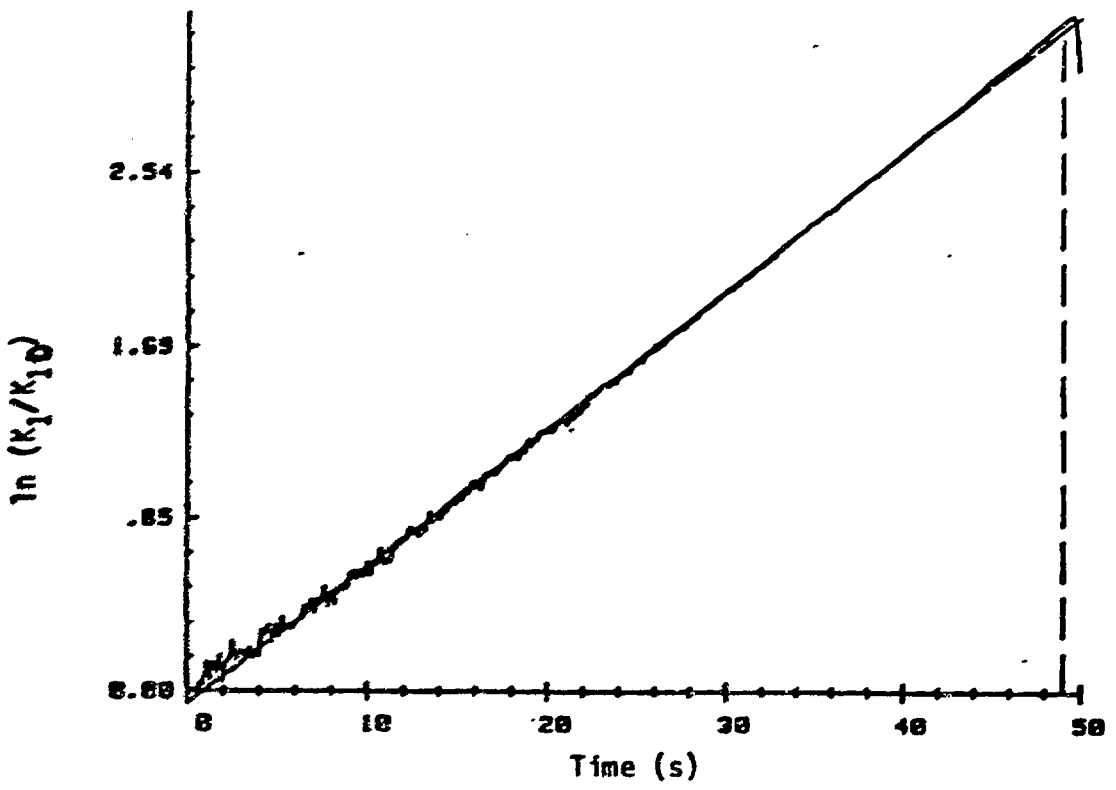


Figure 3. Typical Response Function for a High Reynolds Number, Liquid-Filled System

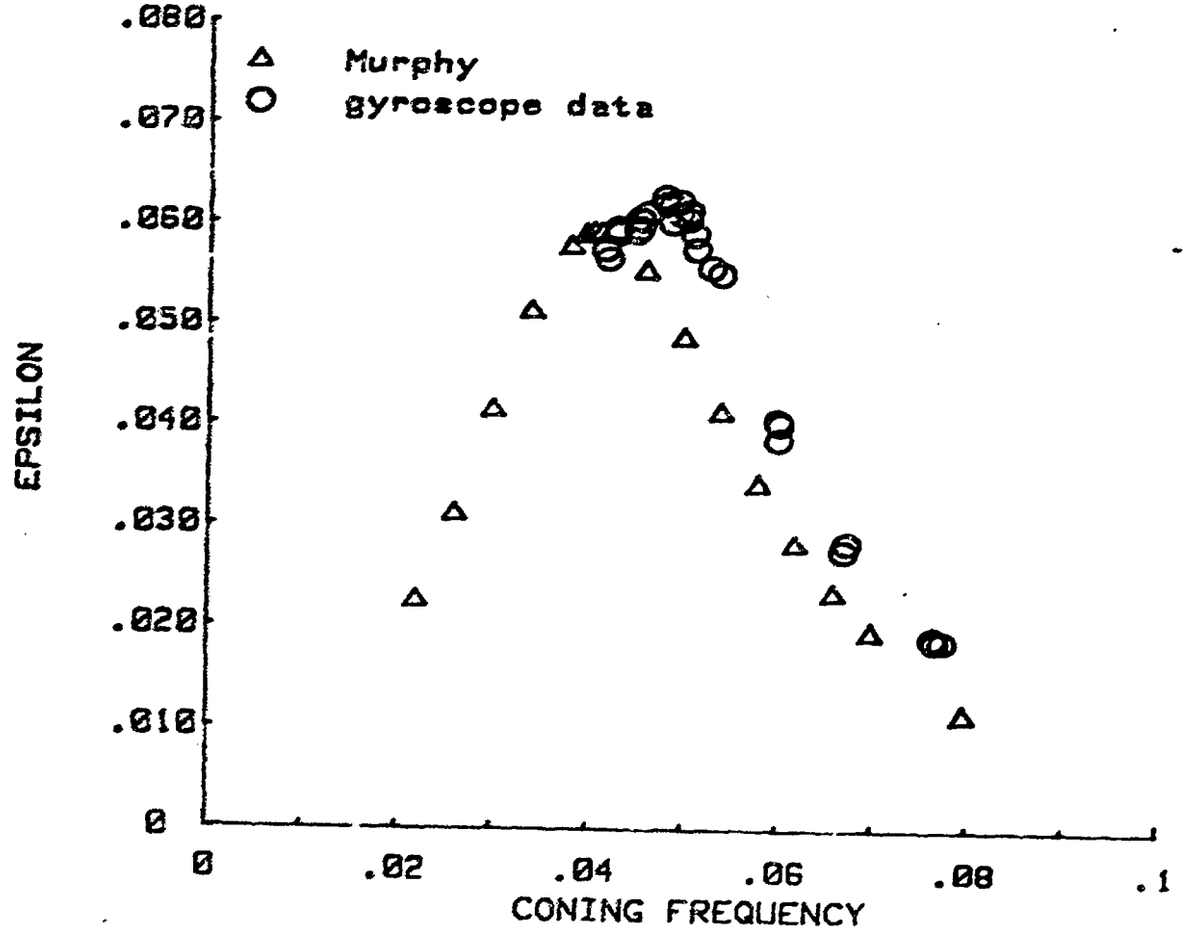


Figure 4a. Comparison of Theory by Murphy (Ref. 4 ) and Gyroscope Data: Fill Ratio 100%, c/a = 1.042, Re = 12,400, $I_x$ = 7.94x10$^5$ gm-cm$^2$, n = 1, j = 0

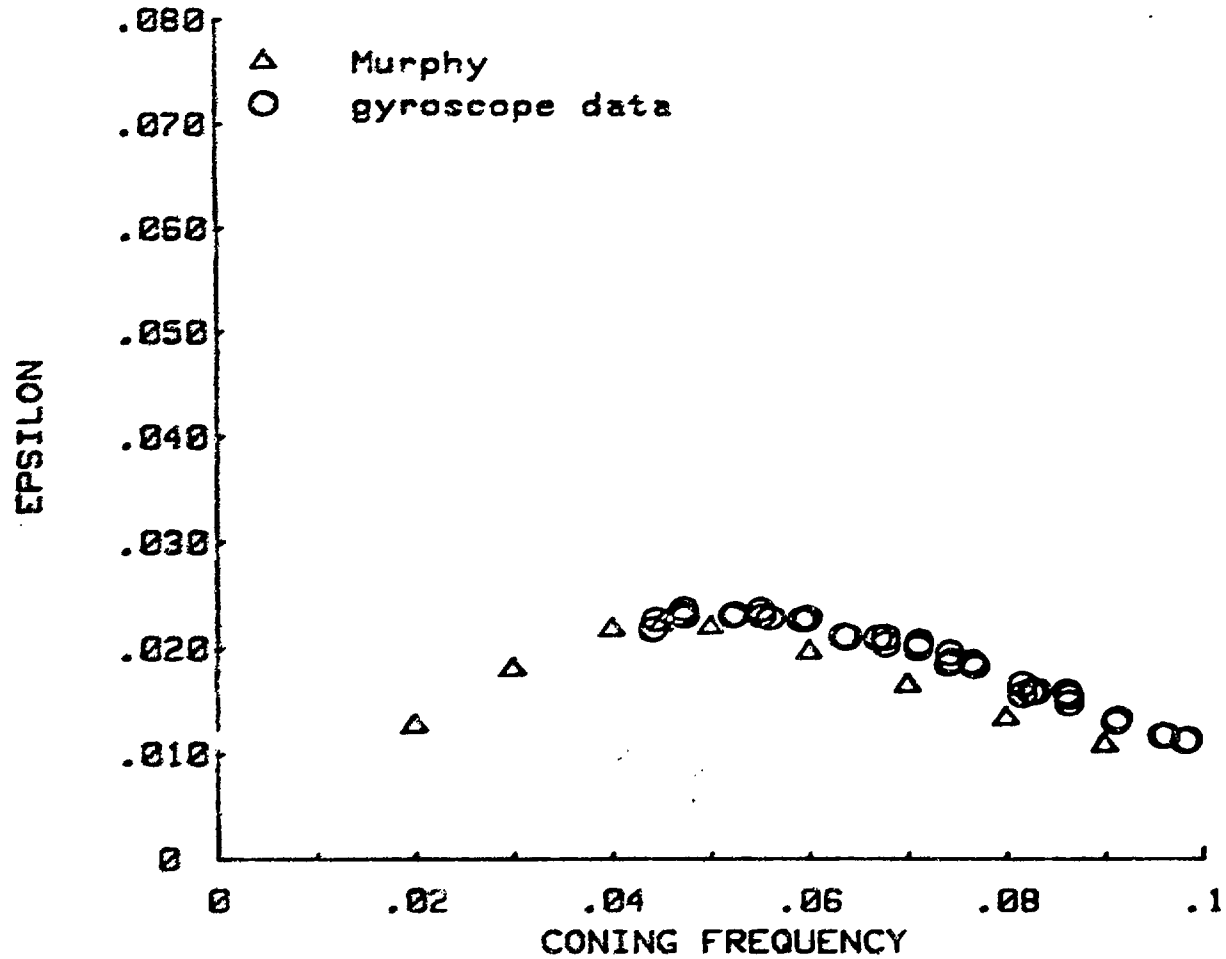


Figure 4b. Comparison of Theory by Murphy (Ref. 4) and Gyroscope Data: Fill Ratio 100%, c/a = 1.042, Re = 2,400, $I_x$ = 10.46x10$^5$ gm-cm$^2$, n = 1, j = 0

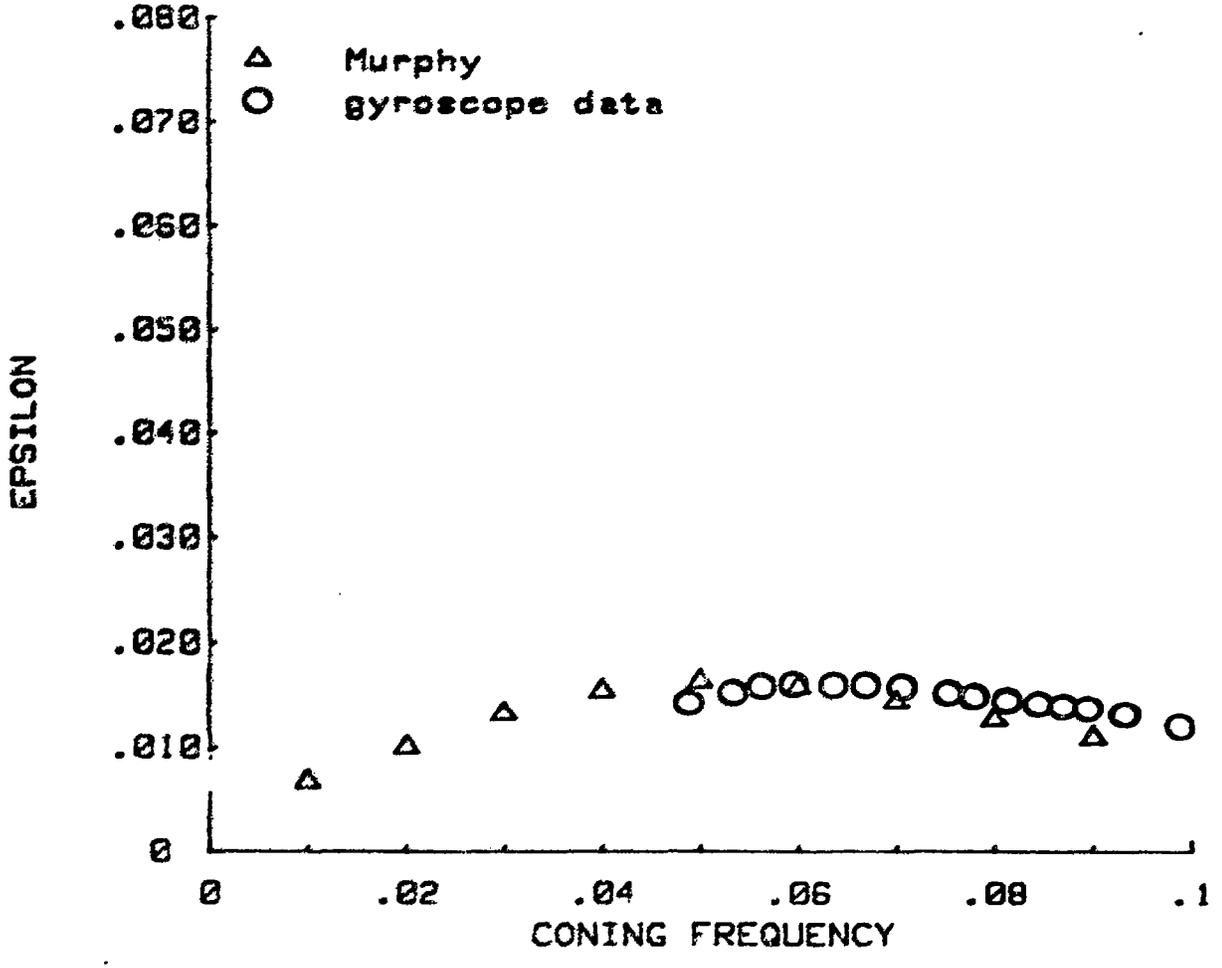


Figure 4c. Comparison of Theory by Murphy (Ref. 4 ) and Gyroscope Data: Fill Ratio 100%, c/a = 1.042, Re = 1,260, $I_x$ = 10.46x10$^5$ gm-cm$^2$, n = 1, j = 0

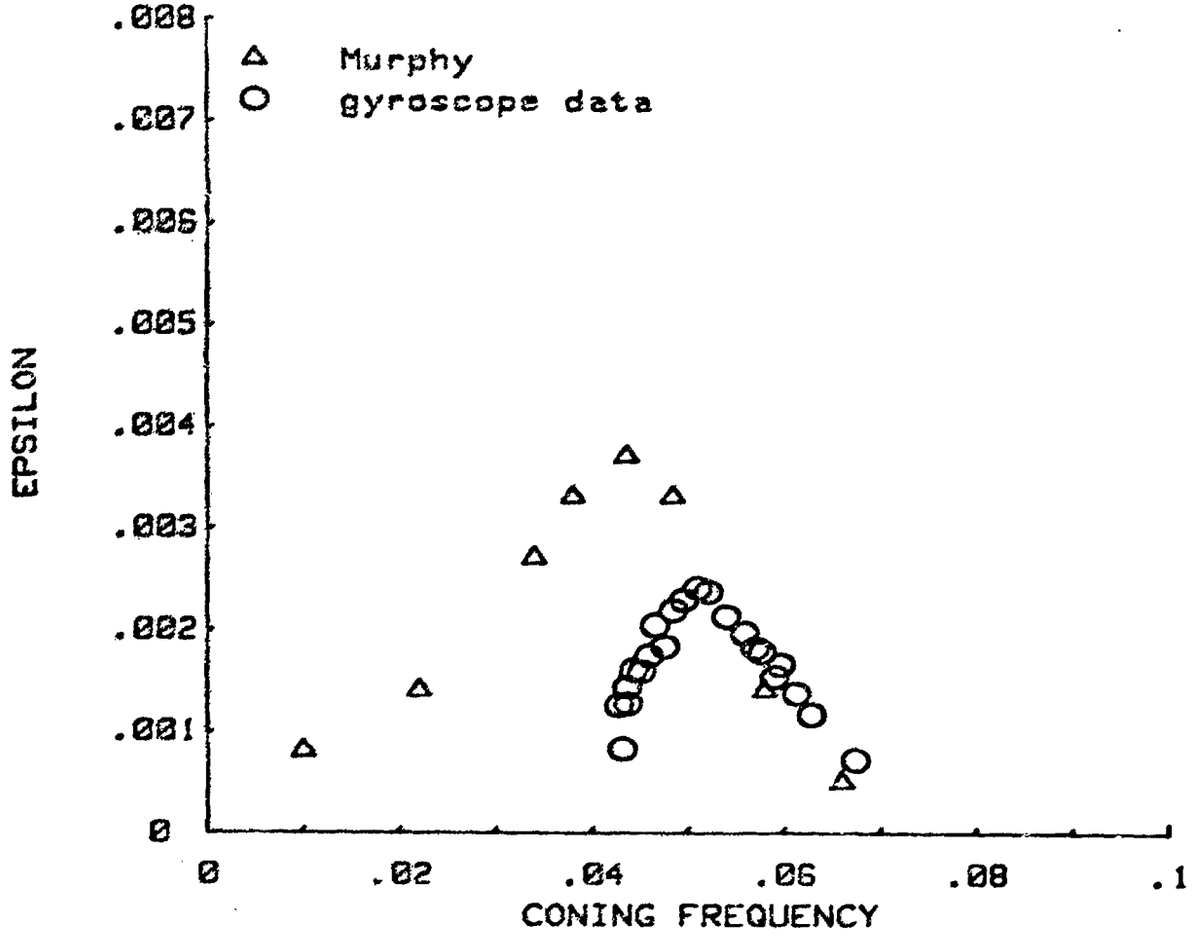


Figure 5a. Comparison of Theory by Murphy (Ref. 4) and Gyroscope Data: Fill Ratio 100%, c/a = 3.126, Re = 5,210, $I_x$ = 8.23x10$^5$ gm-cm$^2$, n = 1, j = 1

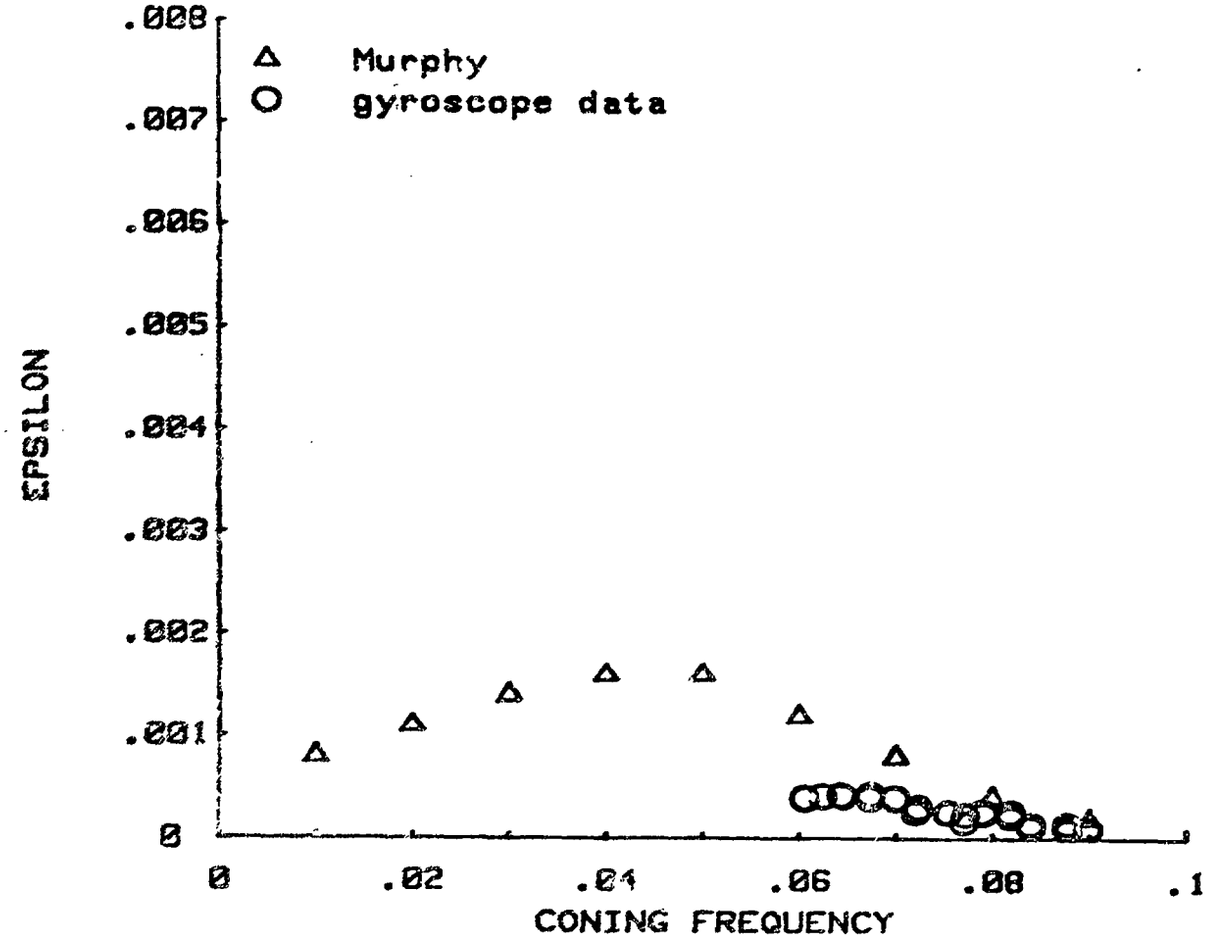


Figure 5b. Comparison of Theory by Murphy (Ref. 4) and Gyroscope Data: Fill Ratio 100%, c/a = 3.126, Re = 1,010, $I_x = 10.76 \times 10^5$ gm·cm$^2$, n = 1, j = 1

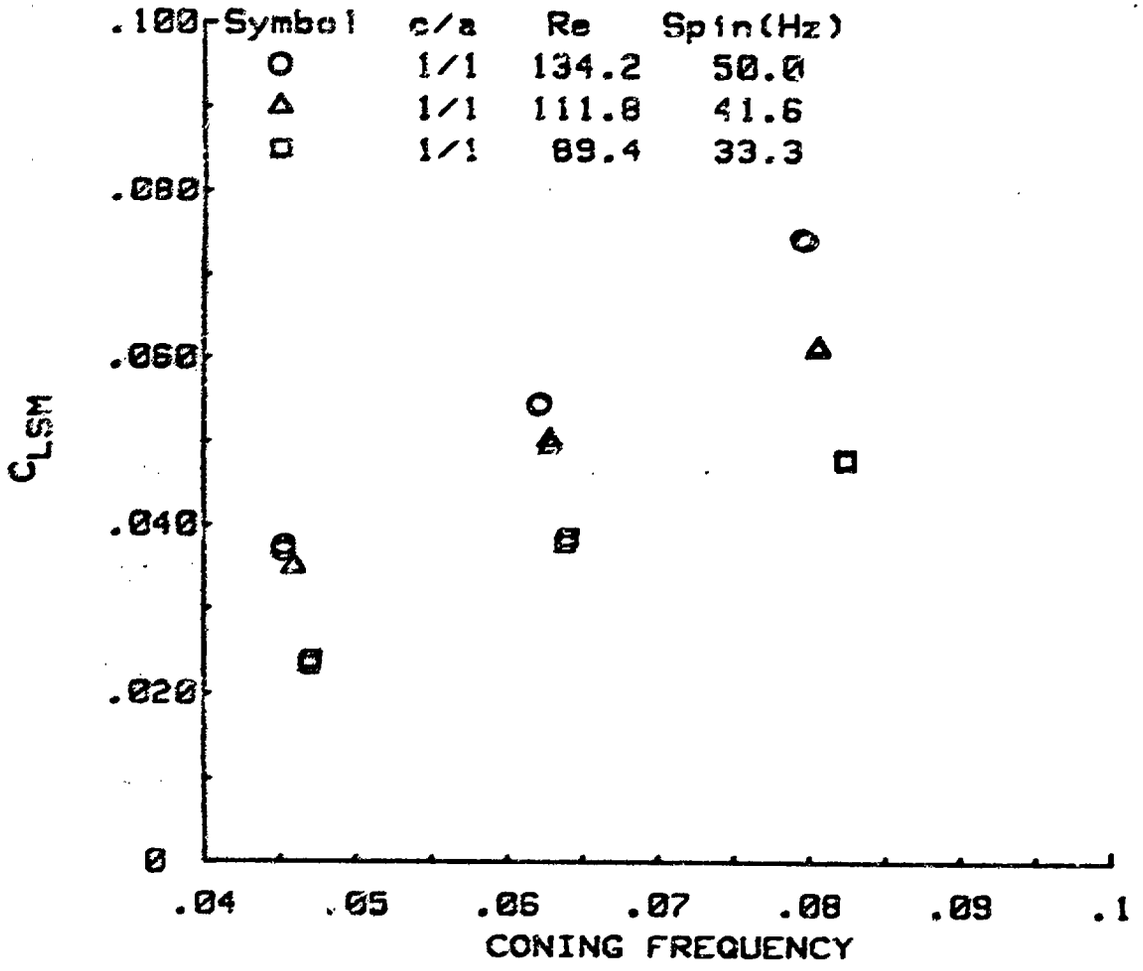


Figure 6a. Liquid Side Moment Coefficient ($C_{LSM}$) Versus Coning Frequency ($\tau$) for c/a of 1/1 With a Viscosity Ratio of 10,000

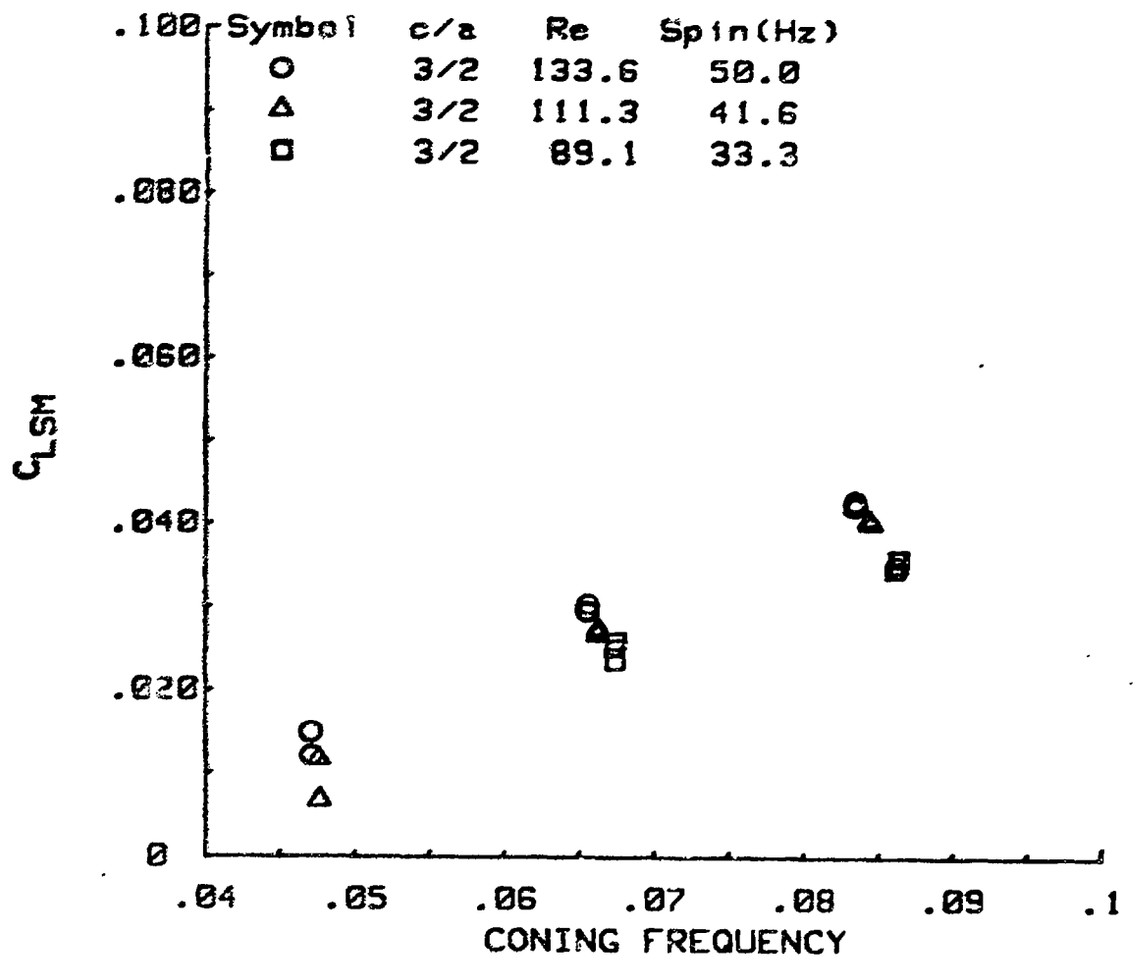


Figure 6b. Liquid Side Moment Coefficient ($C_{LSM}$) Versus Coning Frequency ($\tau$) for c/a of 3/2 With a Viscosity Ratio of 10,000

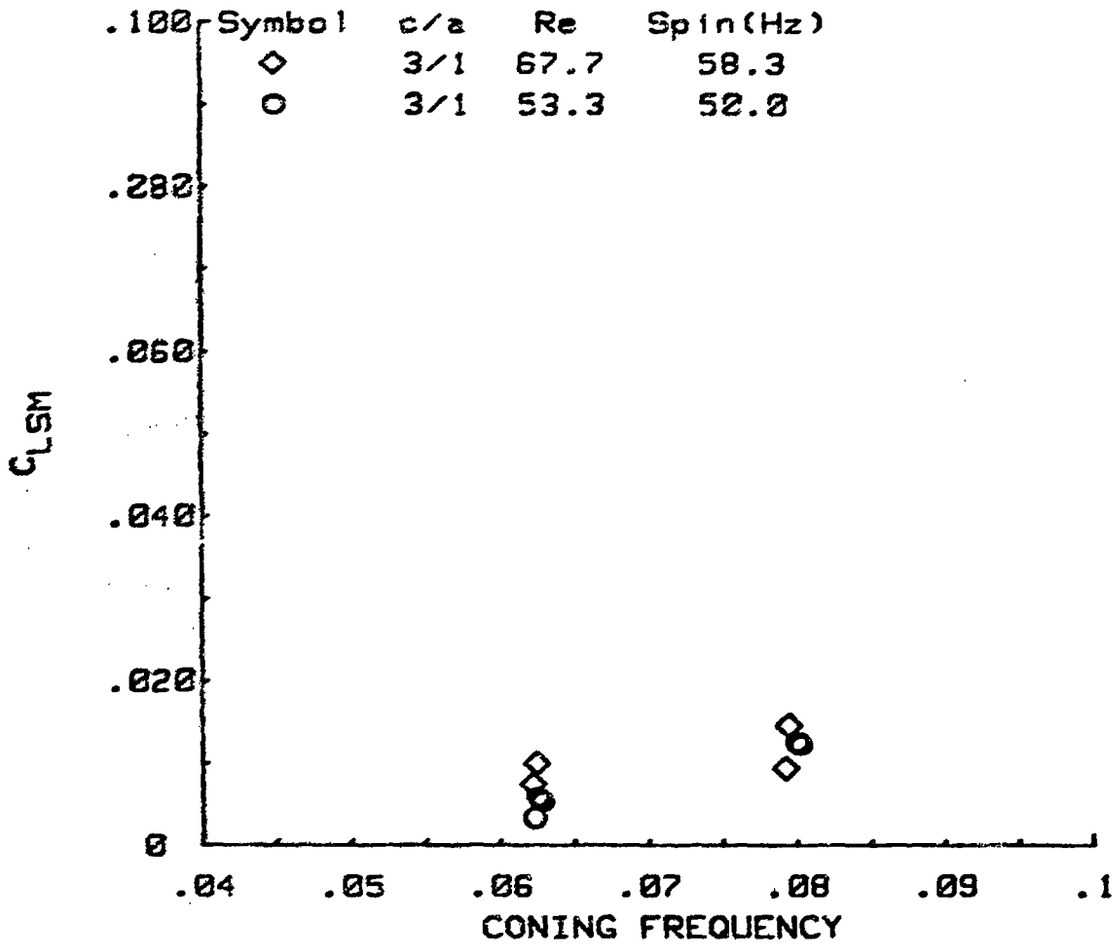


Figure 6c. Liquid Side Moment Coefficient ($C_{LSM}$) Versus Coning Frequency ($\tau$) for c/a of 3/1 With a Viscosity Ratio of 10,000

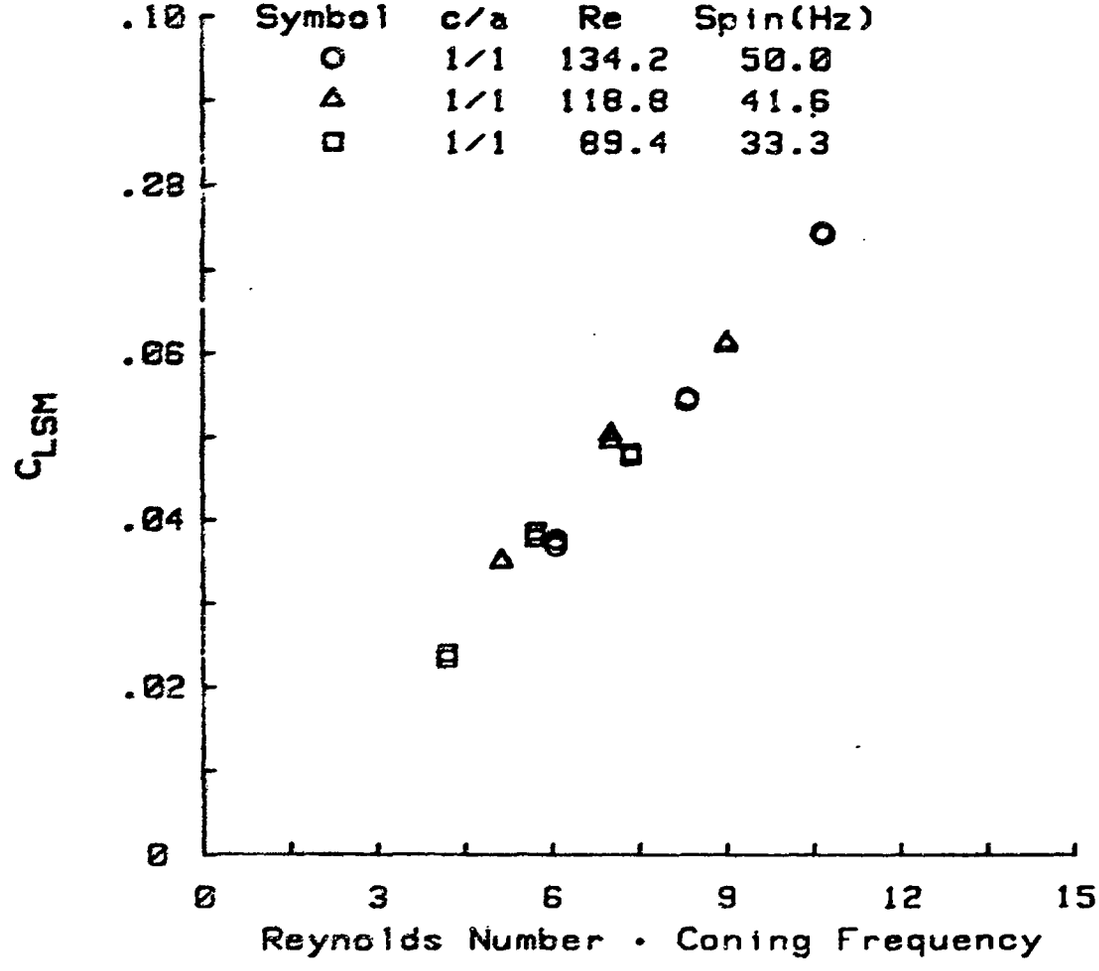


Figure 6d. Liquid Side Moment Coefficient ($C_{LSM}$) Versus Re • τ for c/a of 1/1 With a Viscosity Ratio of 10,000

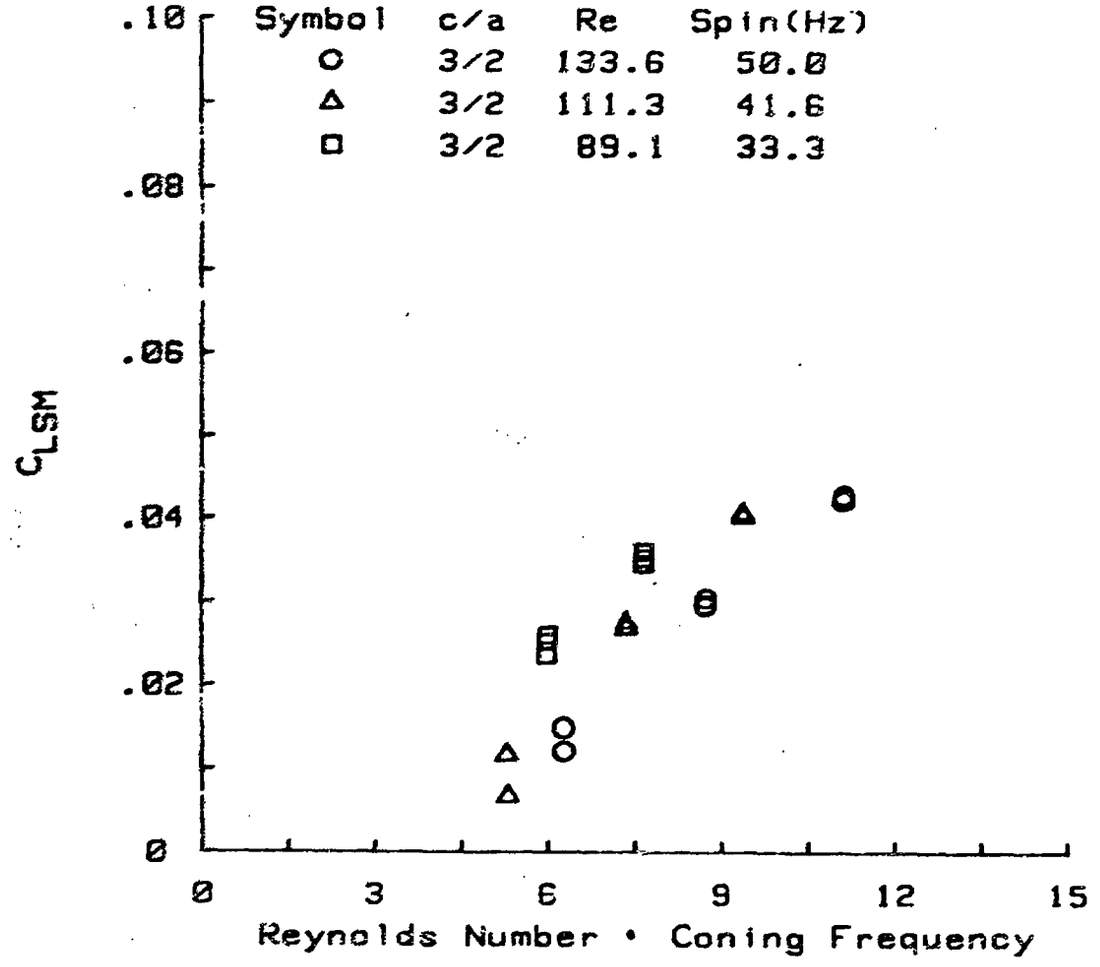


Figure 6e. Liquid Side Moment Coefficient ($C_{LSM}$) Versus Re • $\tau$ for c/a of 3/2 With a Viscosity Ratio of 10,000

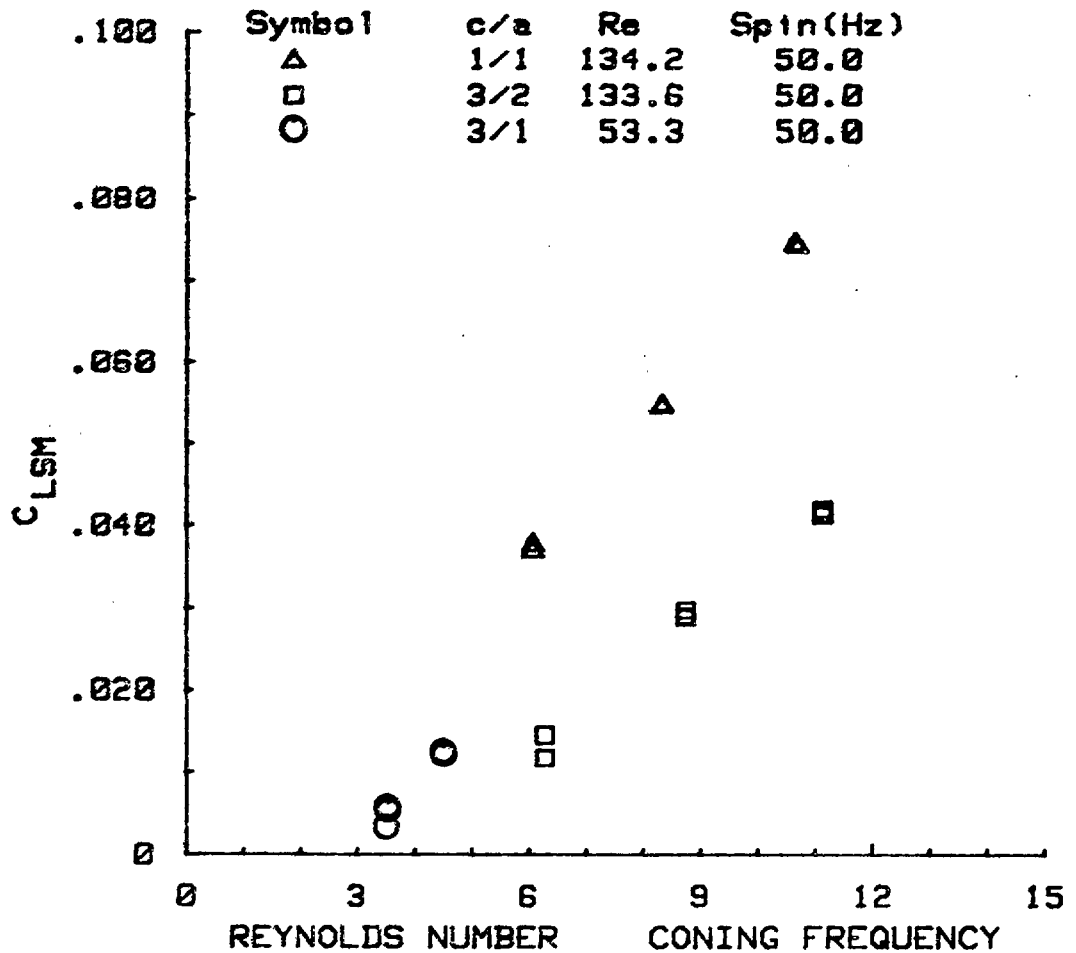


Figure 6f. Liquid Side Moment Coefficient ($C_{LSM}$) Versus Re · $\tau$ for c/a's of 1/1, 3/2, and 3/1 with a Viscosity Ratio of 10,000

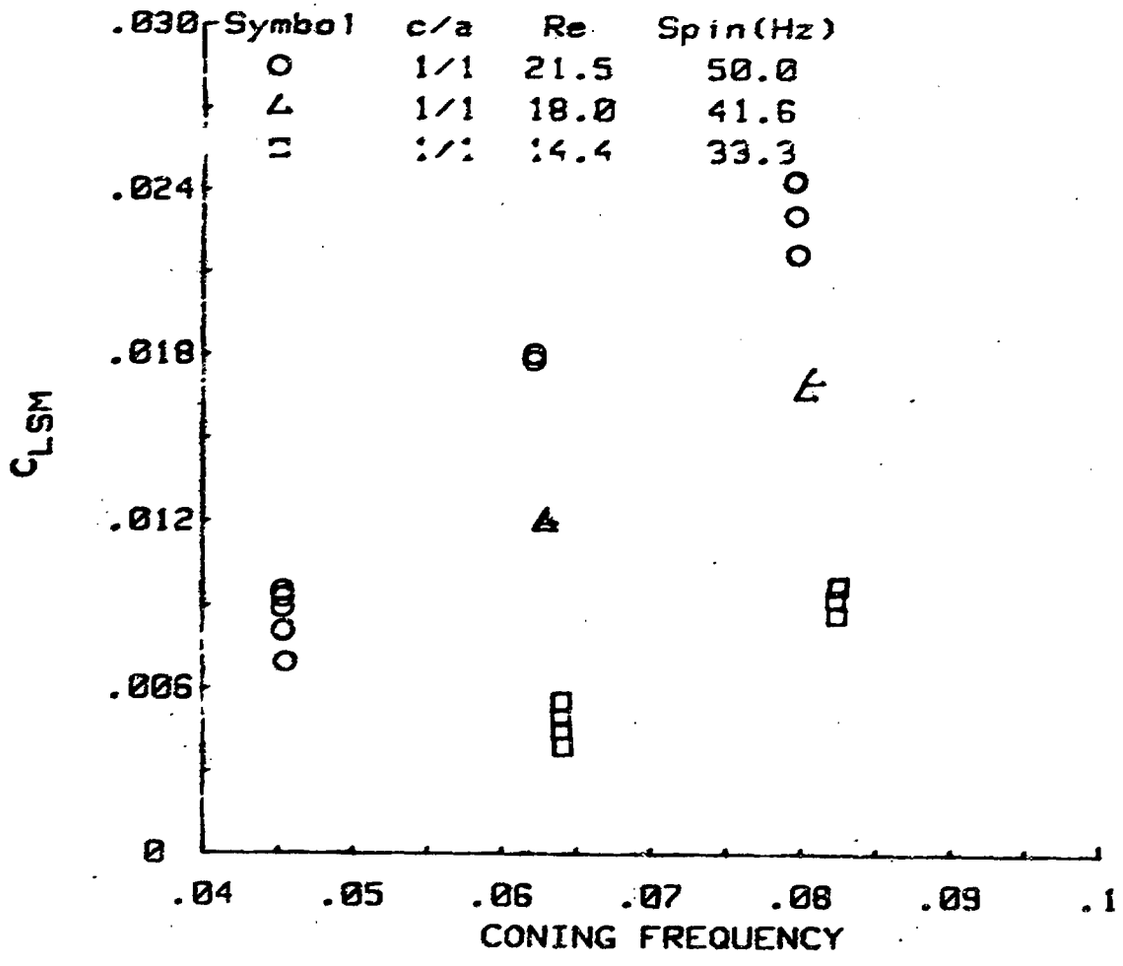


Figure 7a. Liquid Side Moment Coefficient ($C_{LSM}$) Versus Coning Frequency ($\tau$) for c/a of 1/1 and a Viscosity Ratio of 60,000

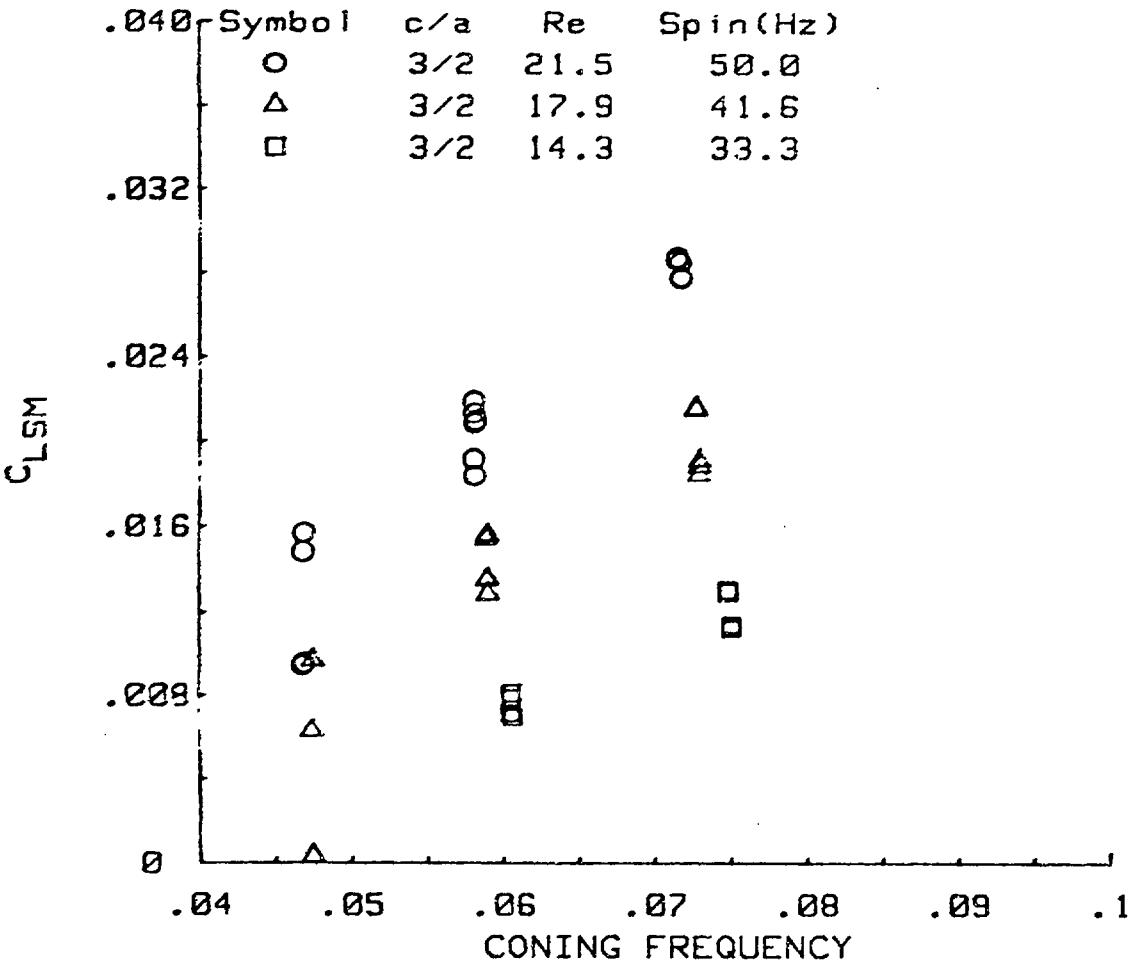


Figure 7b. Liquid Side Moment Coefficient ($C_{LSM}$) Versus Coning Frequency ($\tau$) for c/a of 3/2 and a Viscosity Ratio of 60,000

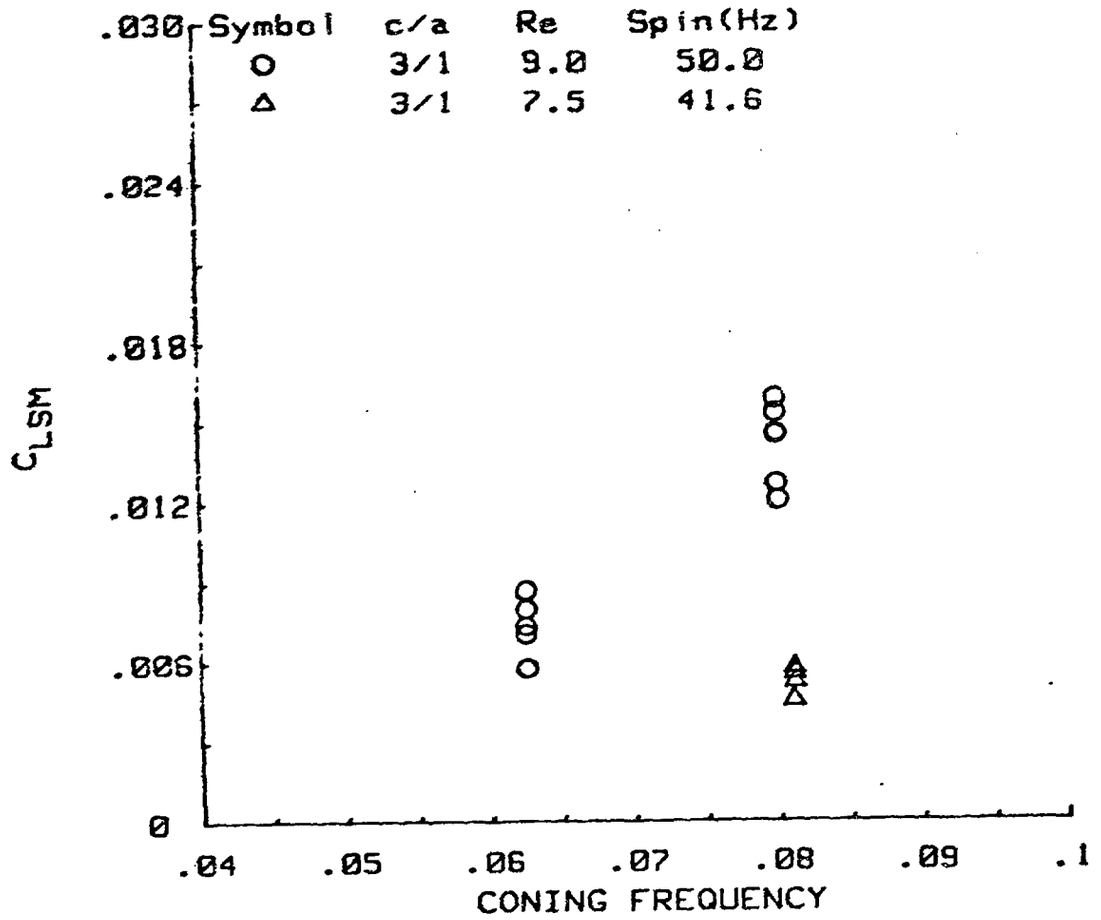


Figure 7c. Liquid Side Moment Coefficient ($C_{LSM}$) Versus Coning Frequency ($\tau$) for c/a of 3/1 and a Viscosity Ratio of 60,000

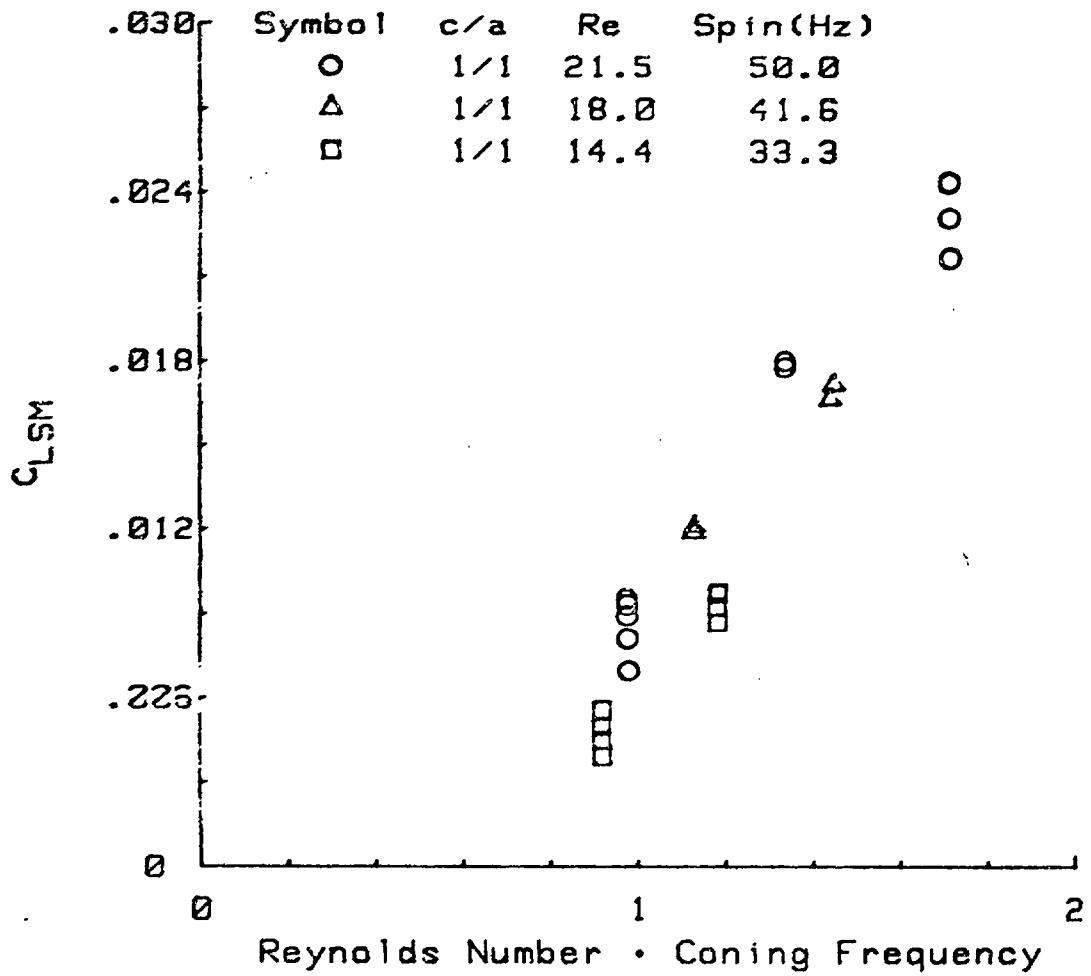


Figure 7d. Liquid Side Moment Coefficient ($C_{LSM}$) Versus Coning Frequency ($\tau$) for c/a of 1/1 and a Viscosity Ratio of 60,000

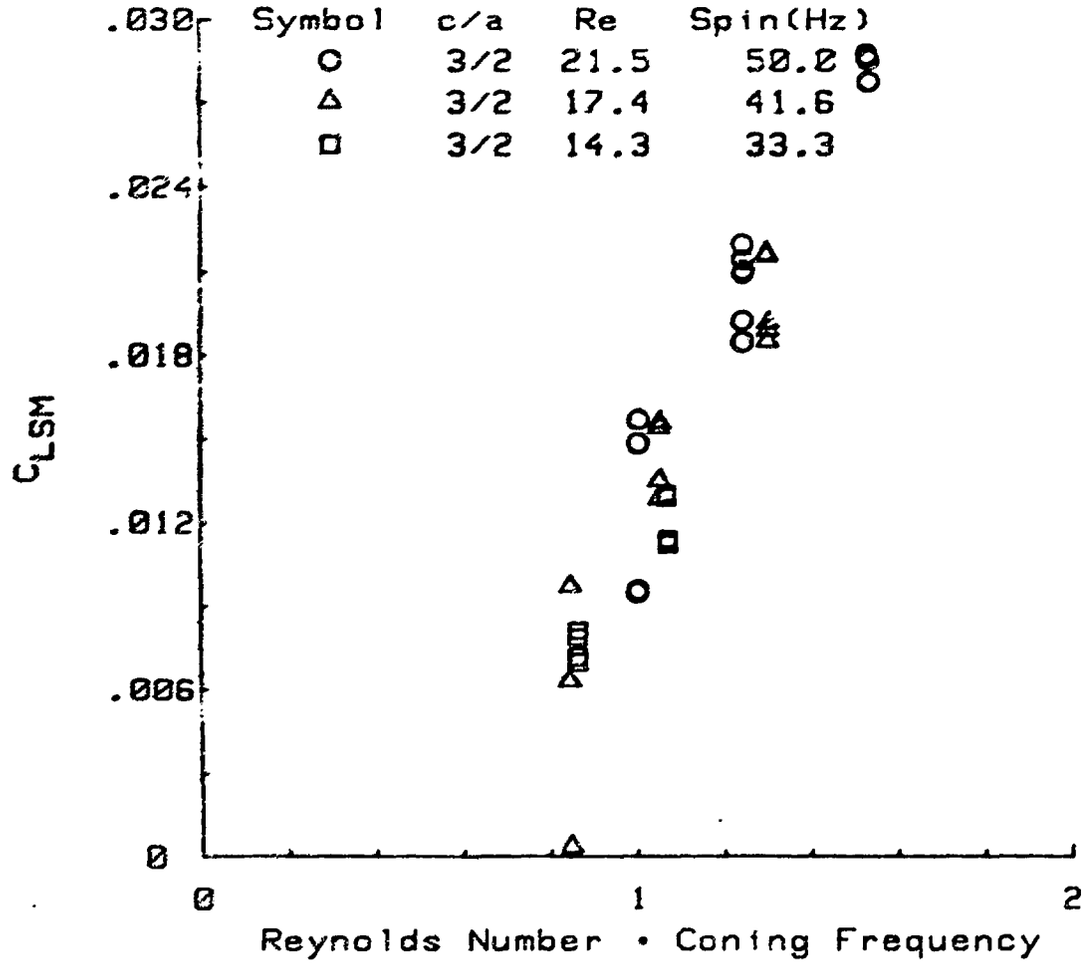


Figure 7e. Liquid Side Moment Coefficient ($C_{LSM}$) Versus Re • $\tau$ for c/a of 3/2 and a Viscosity Ratio of 60,000

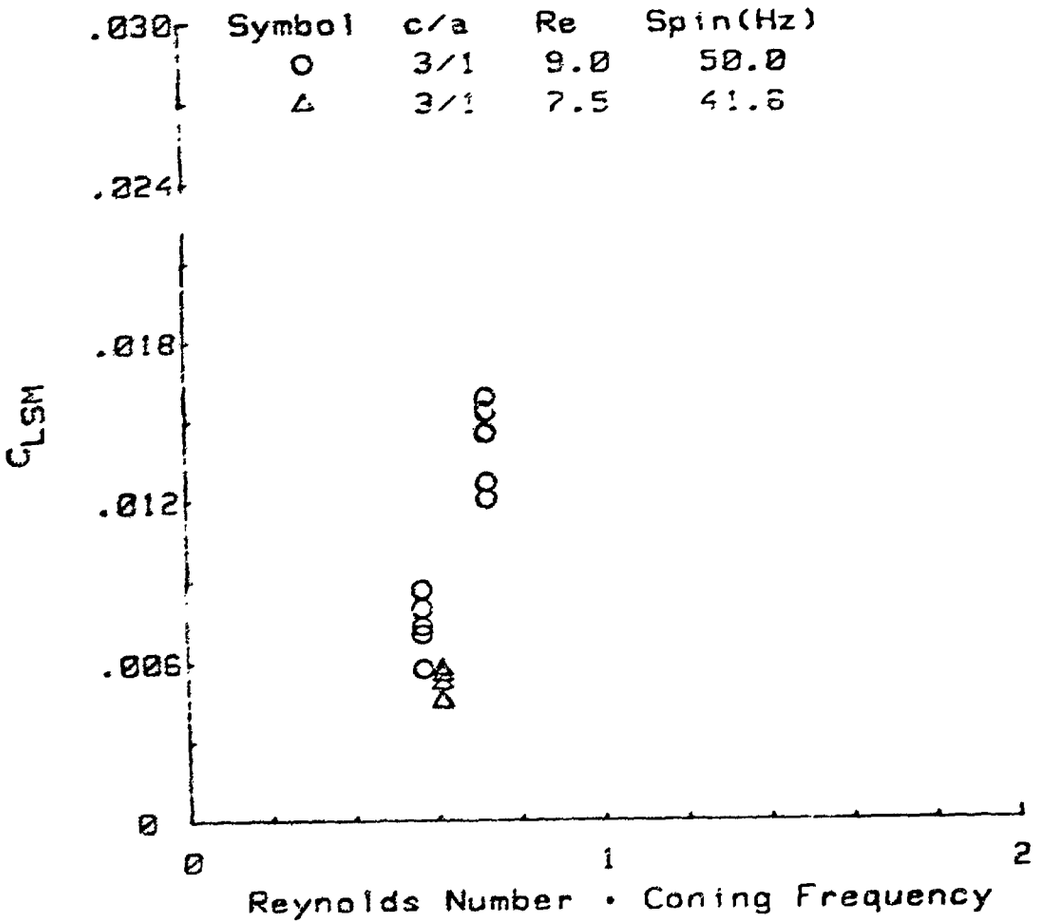


Figure 7f. Liquid Side Moment Coefficient ($C_{LSM}$) Versus Re • $\tau$ for c/a of 3/1 and a Viscosity Ratio of 60,000

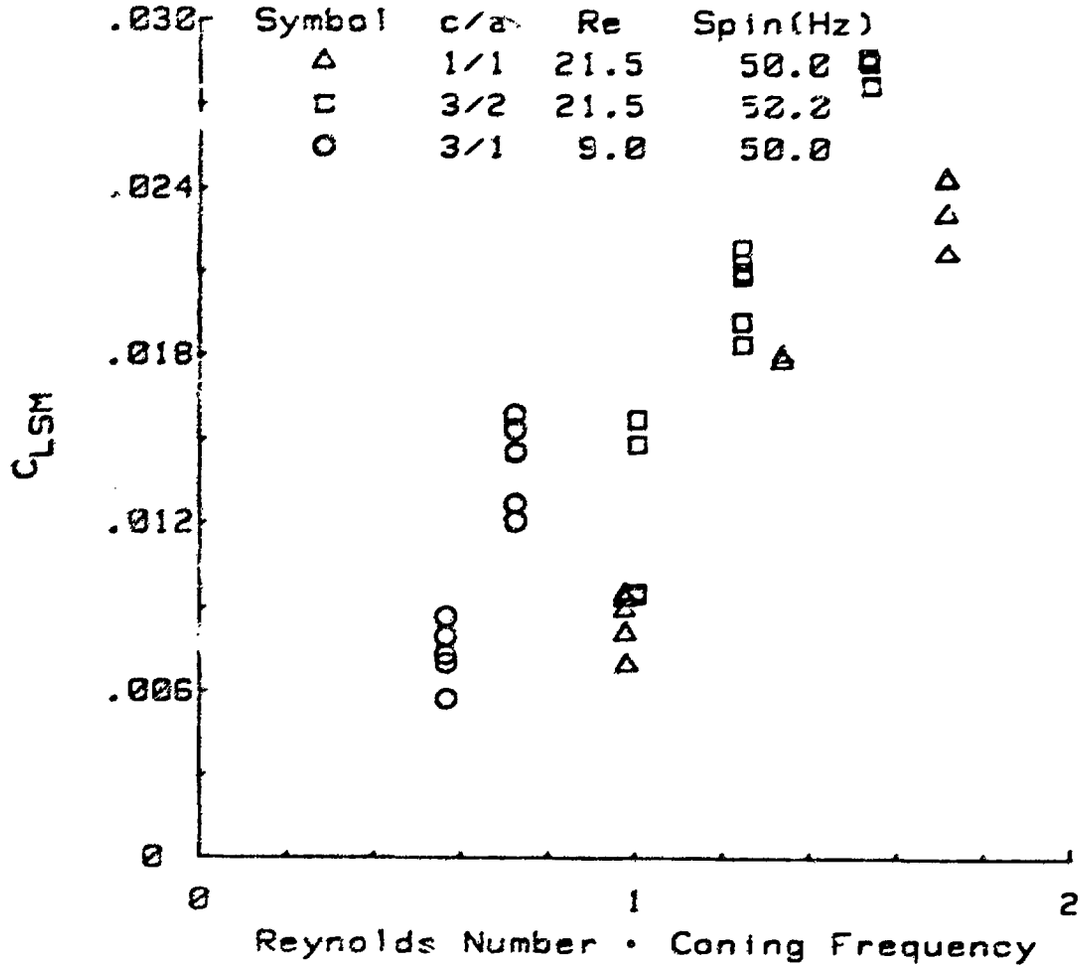


Figure 7g. Liquid Side Moment Coefficient ($C_{LSM}$) Versus Re • $\tau$ for c/a's of 1/1, 3/2, and 3/1 With a Viscosity Ratio of 60,000

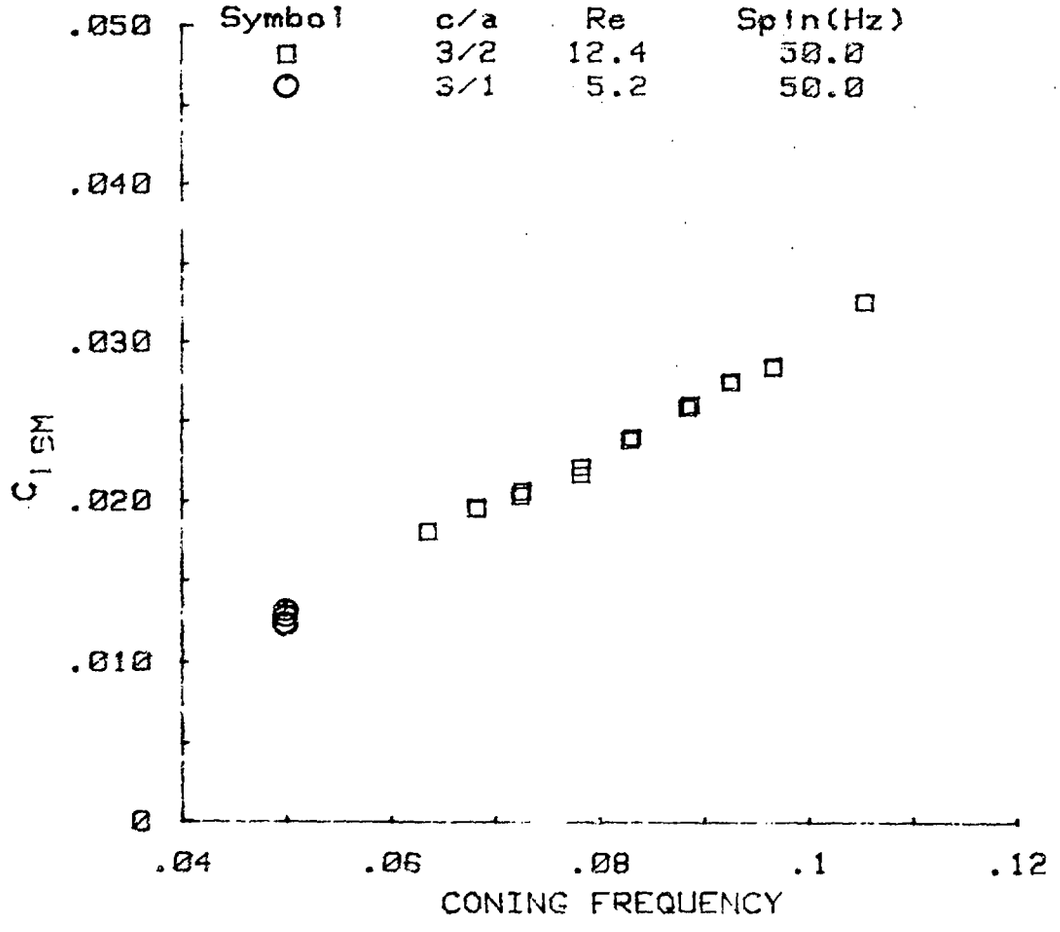


Figure 8. Liquid Side Moment Coefficient ($C_{LSM}$) Versus Coning Frequency ($\tau$) for c/a's of 3/1 and 3/2 and a Viscosity Ratio of 100,000

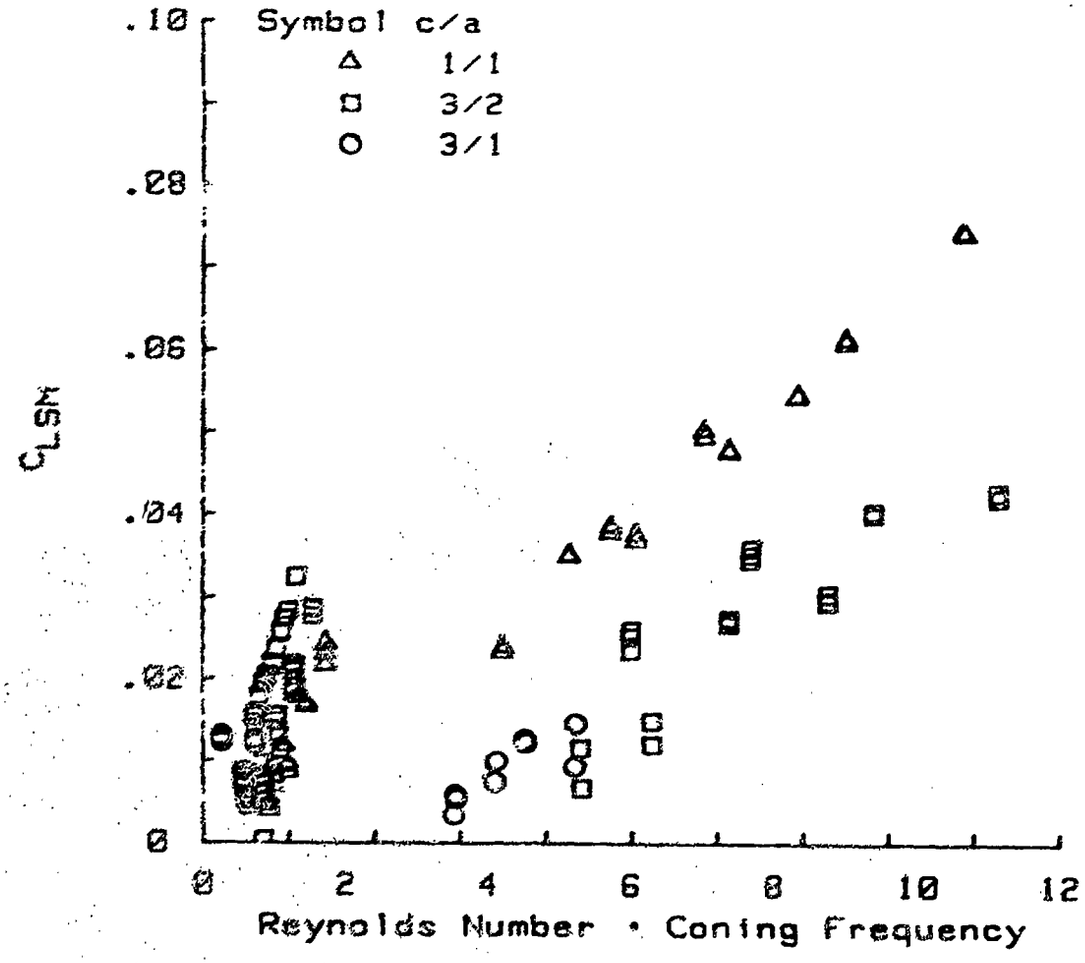


Figure 9. Correlation of all Data with Viscosity Ratios of 100,000, 60,000, and 10,000 for $C_{LSM}$ Versus Re • τ

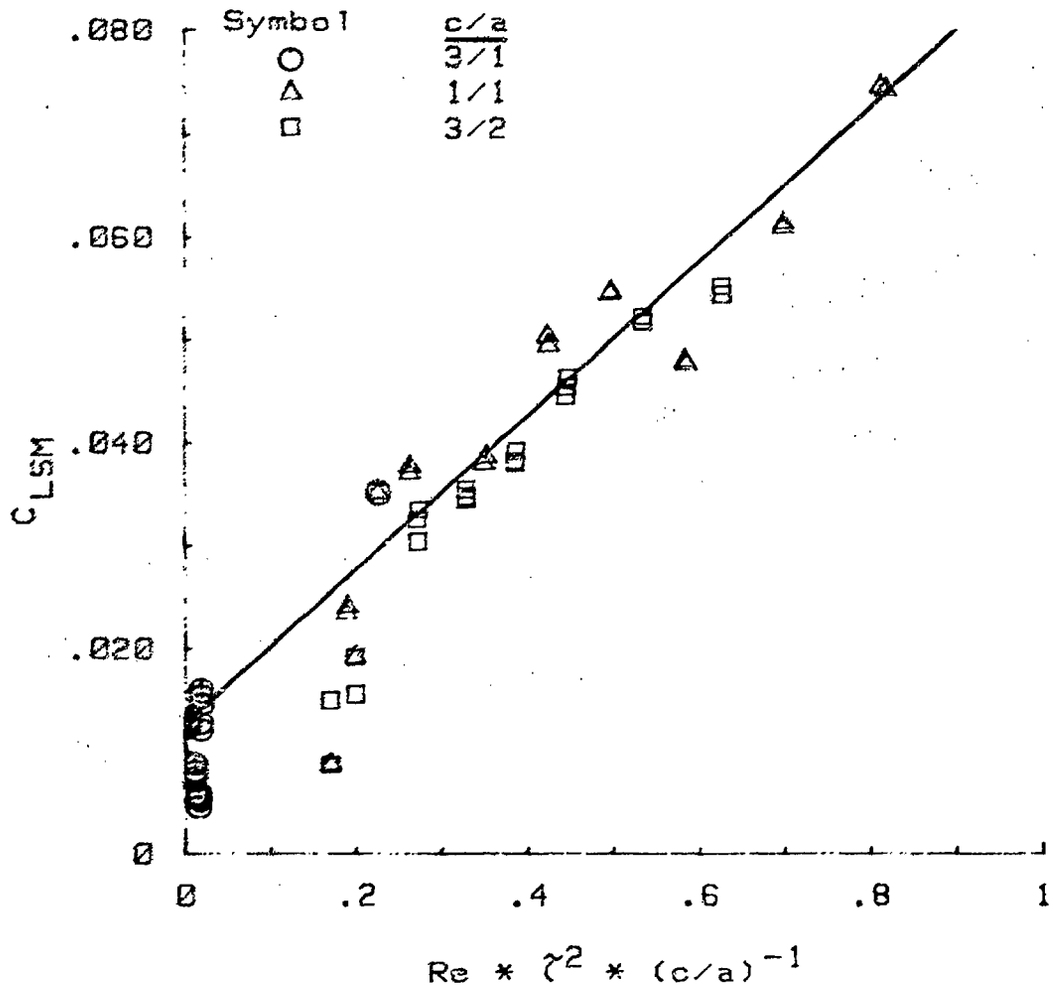


Figure 10. Correlation of all Data for Viscosity Ratios of 100,000, 60,000, and 10,000 for $C_{LSM}$ Versus Re · $\tau^2$ · $(c/a)^{-1}$

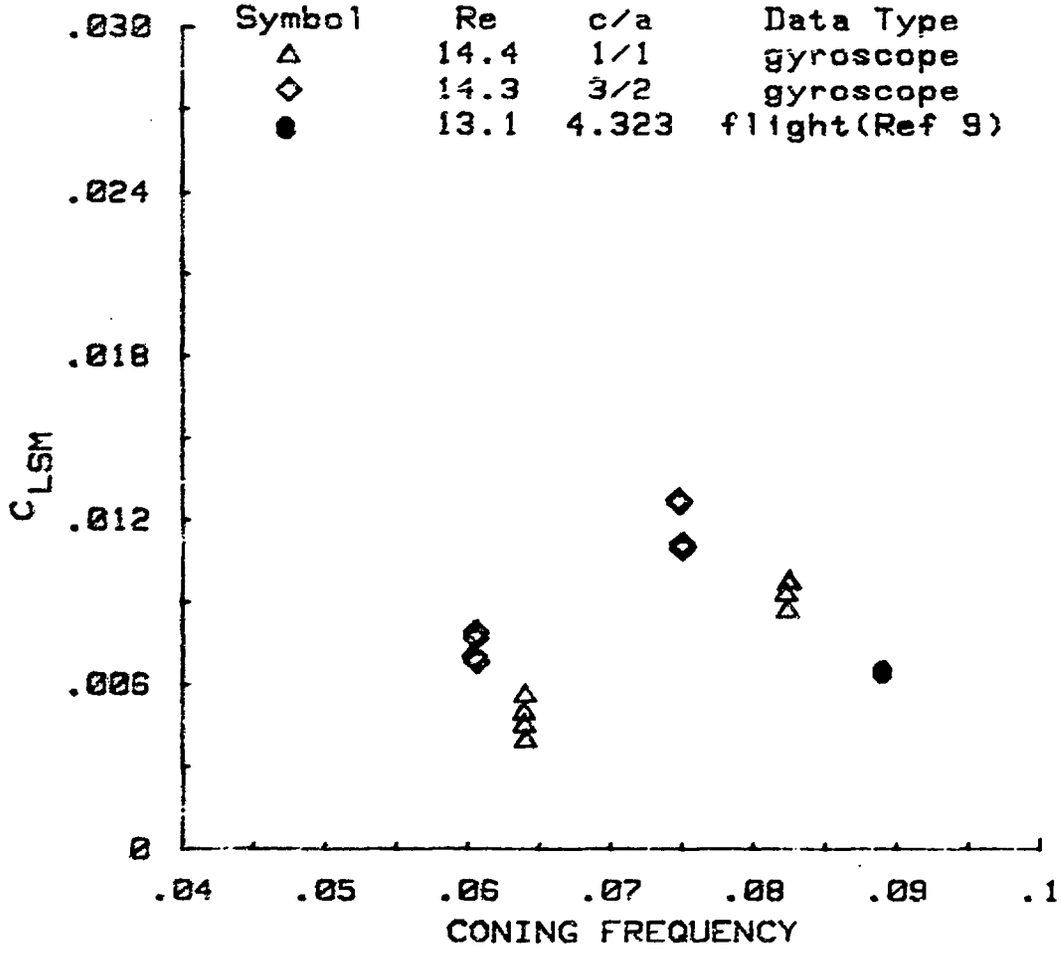


Figure 11. Comparison of $C_{LSM}$ for Laboratory Gyroscope and Projectile Flight for Re ≈ 14

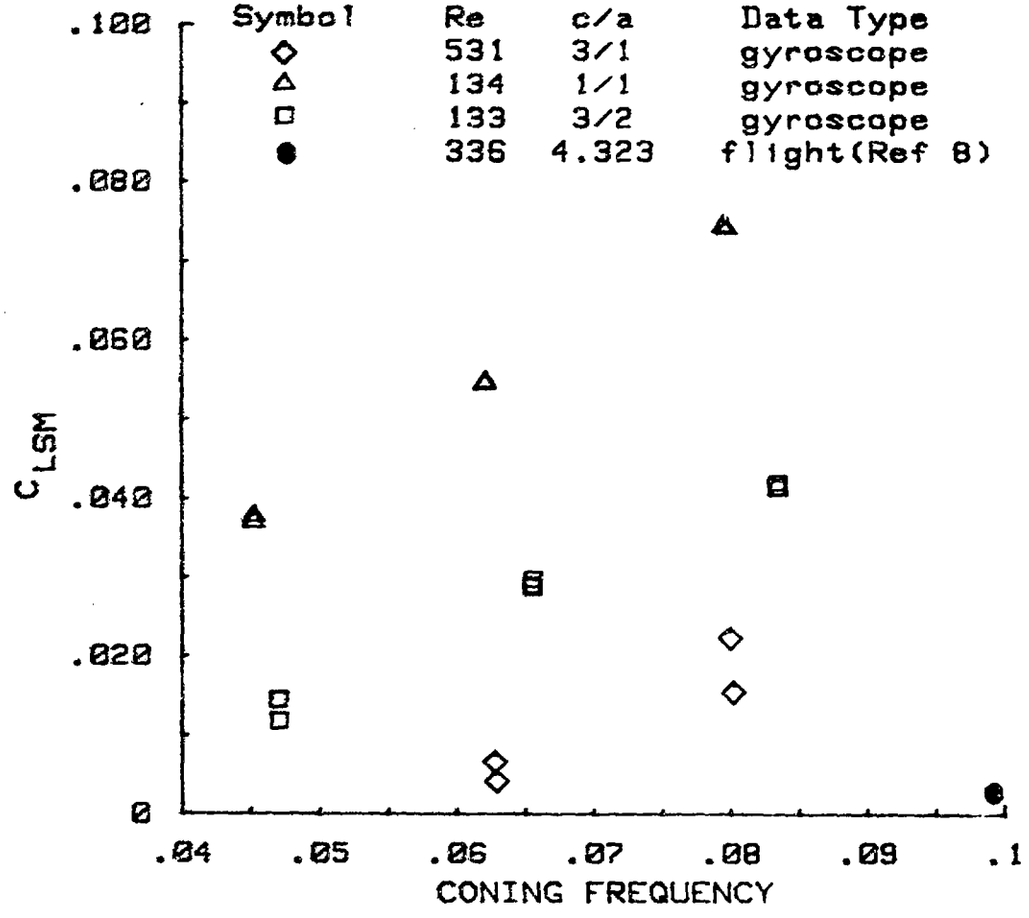


Figure 12. Comparison of $C_{LSM}$ for Laboratory Gyroscope and Projectile Flight for 133 < Re < 531

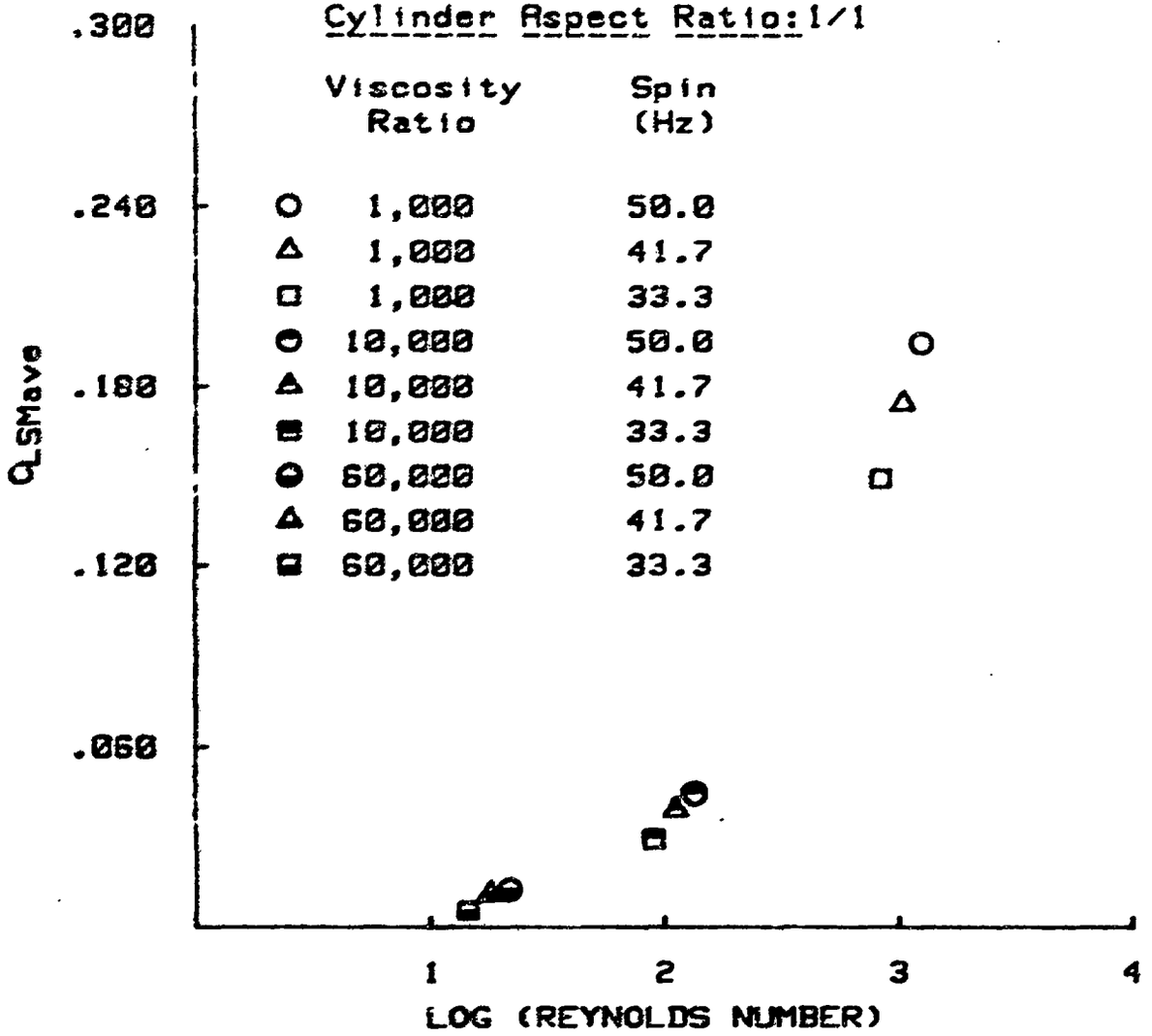


Figure 13a. Average $C_{LSM}$ Versus $Log_{10}$ (Re) for c/a = 1/1

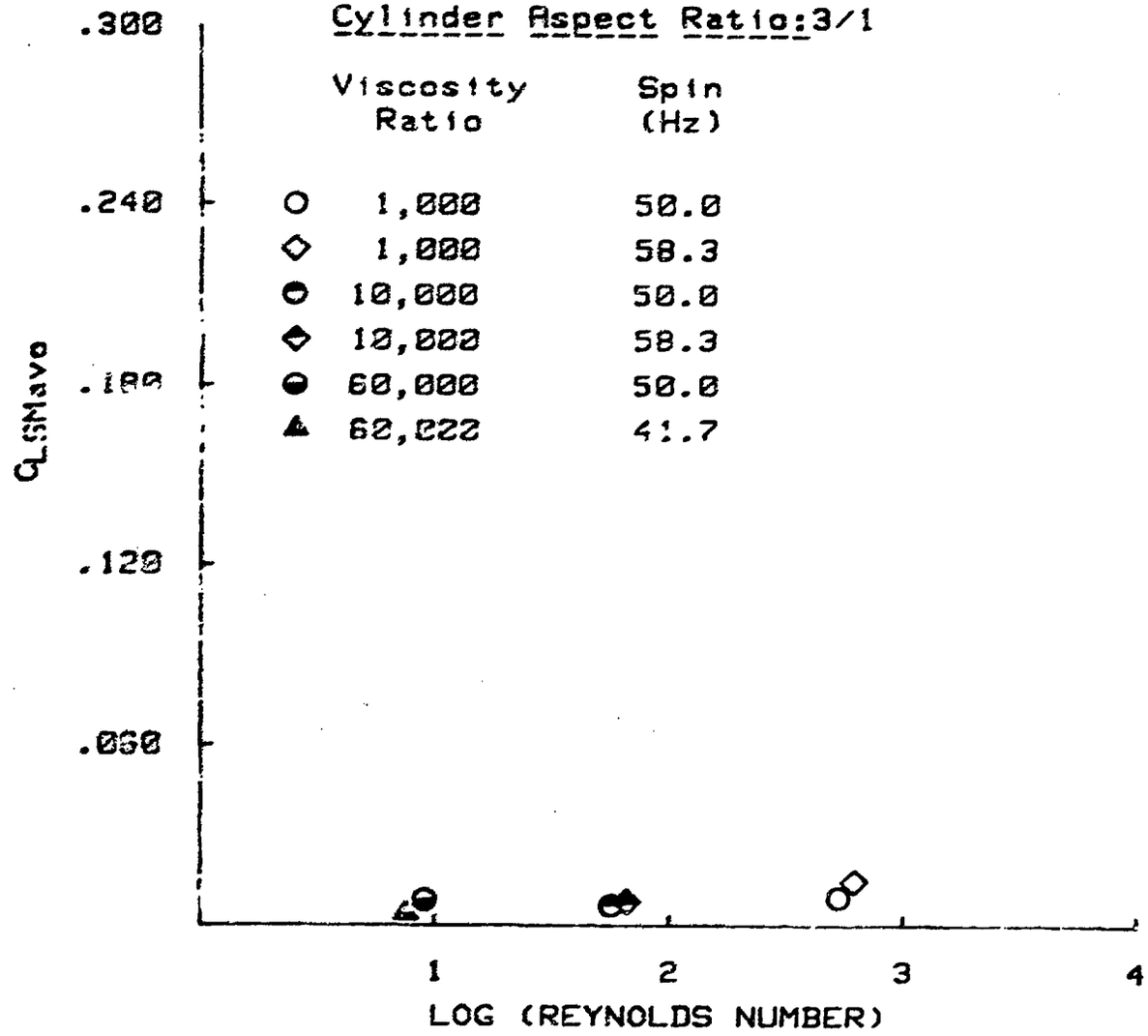


Figure 13b. Average $C_{LSM}$ Versus $Log_{10}$ (Re) for c/a = 3/1

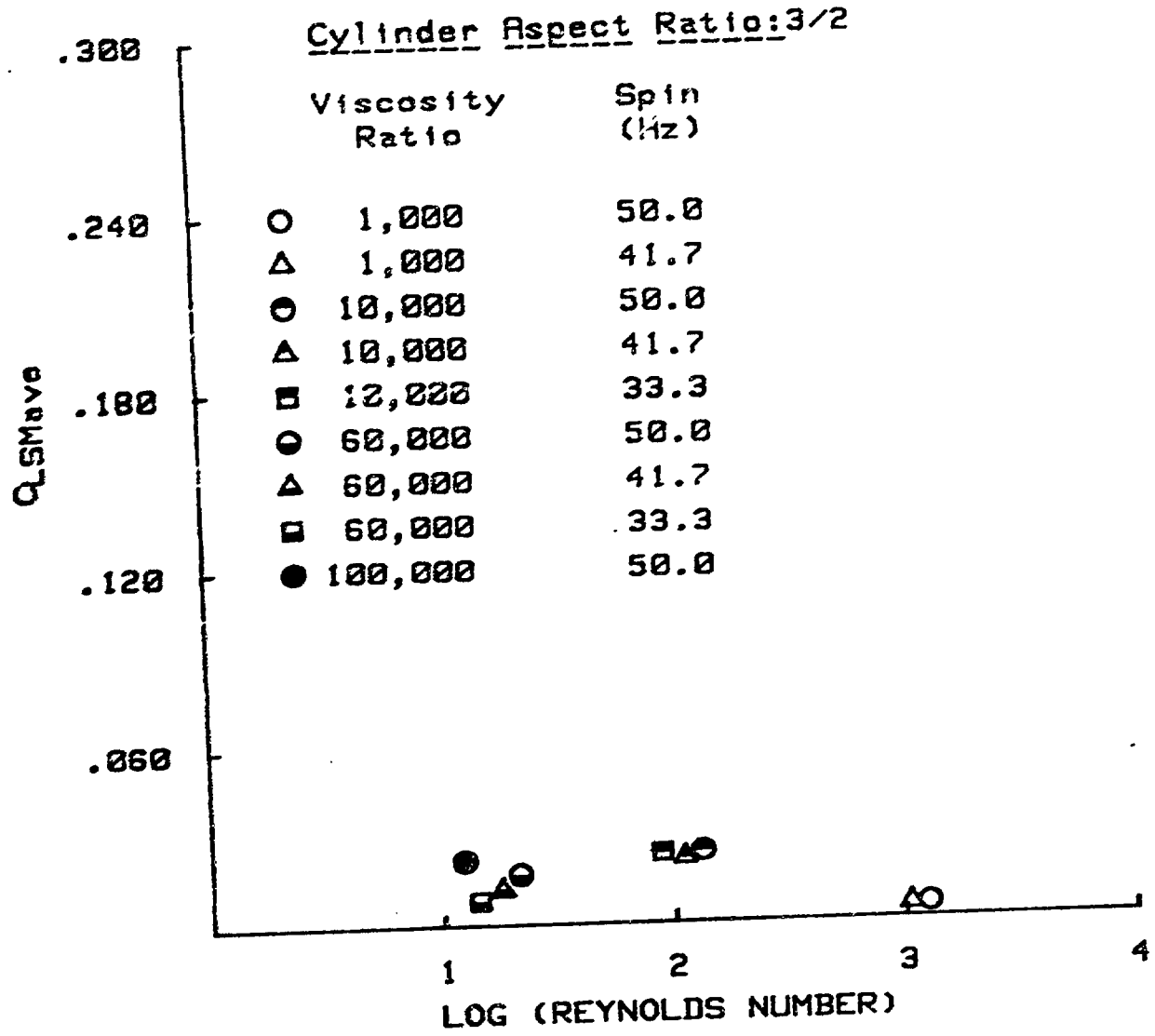


Figure 13c. Average $C_{LSM}$ Versus $Log_{10}$ (Re) for c/a = 3/2

REFERENCES


1. K. Stewartson, "On the Stability of a Spinning Top Containing Liquid," Journal of Fluid Mechanics, Vol. 5, 1959, pp. 577-592.

2. E. H. Wedemeyer, "Viscous Corrections to Stewartson's Stability Criterion," BRL Report No. 1325, June 1966 (AD 489687).

3. B. G. Karpov, "Liquid-Filled Gyroscope: The Effect of Reynolds Number on Resonance," BRL Report No. 1302, October 1965 (AD 479430).

4. Charles H. Murphy, "Angular Motion of a Spinning Projectile With a Viscous Liquid Payload," BRL Memorandum Report No. ARBRL-MR-03194, August 1982 (AD A118676).

5. Nathan Gerber and Raymond Sedney, "Moment on a Liquid-Filled Spinning and Nutating Projectile: Solid Body Rotation," BRL Technical Report No. ARBRL-TR-02470 (AD A125332).

6. W. P. D'Amico and M. C. Miller, "Flight Instability Produced by a Rapidly Spinning, Highly Viscous Liquid," Journal of Spacecraft and Rockets, Vol. 16, No. 1, January-February 1979, pp. 62-64.

7. Miles C. Miller, "Flight Instabilities of Spinning Projectiles Having Non-Rigid Payloads," Journal of Guidance Control and Dynamics, Vol. 5, March-April 1982, pp. 151-157.

8. W. P. D'Amico, W. H. Clay, and A. Mark, "Diagnostic Tests for Wick-Type Payloads and High Viscosity Liquids," BRL Memorandum Report No. ARBRL-MR-02913, April 1979 (AD A072812).

9. W. P. D'Amico and W. H. Clay, "High Viscosity Liquid Payload Yawsonde Data for Small Launch Yaws," BRL Memorandum Report No. ARBRL-MR-03029, June 1980 (AD A088411).

10. Charles H. Murphy, "Free Flight Motion of Symmetric Missiles," BRL Report No. 1216, July 1963 (AD 442757).

11. W. E. Scott and W. P. D'Amico, "Amplitude-Dependent Behavior of a Liquid-Filled Gyroscope," Journal of Fluid Mechanics, Vol. 60, Part 4, 1973, pp. 751-758.

12. Richard D. Whiting, "An Experimental Study of Forced Asymmetric Oscillations in a Rotating Liquid-Filled Cylinder," BRL Technical Report No. ARBRL-TR-02370, October 1981 (AD A107948).

## LIST OF SYMBOLS

| | |
|---|---|
| $a$ | radius of a right-circular cylindrical cavity containing liquid |
| $C_{LIM}$ | liquid in-plane moment coefficient for one-mode coning or spiral motion; the imaginary part of $C_{LM}$ |
| $C_{LIM_j}$ | fast (j=1) and slow (j=2) mode liquid in-plane moment coefficients; the imaginary part of $C_{LM_j}$ |
| $C_{LM_j}$ | fast (j=1) and slow (j=2) mode liquid moment coefficients |
| $C_{LRM}$ | $m_L a^2 \phi^2 \tau_1 K_1^2 C_{LRM}$ |
| $C_{LSM}$ | liquid side moment coefficient for one-mode coning or spiral motion; the real part of $C_{LM}$ |
| $C_{LSM_j}$ | fast (j=1) or slow (j=2) mode liquid side moment coefficients; the real part of $C_{LM_j}$ |
| $C_{M_{p_\alpha}}$ | $\dfrac{\lvert\text{Magnus moment}\rvert}{(1/2)\,\rho S \ell^2\, V\, \dot{\phi}\, \lvert\tilde{\xi}\rvert}$ |
| $C_{M_q} + C_{M_{\dot{\alpha}}}$ | $\dfrac{\lvert\text{sum of the damping moments}\rvert}{(1/2)\,\rho S \ell^2\, V\, \lvert\text{cross spin}\rvert}$ |
| $C_{M_\alpha}$ | $\dfrac{\lvert\text{static moment}\rvert}{(1/2)\,\rho S \ell^2\, V\, \lvert\tilde{\xi}\rvert}$ |
| $C_{N_\alpha}$ | $\dfrac{-\,(\text{normal force})}{(1/2)\,\rho S V^2\, \tilde{\xi}}$ |
| $c$ | one-half the length of the cylindrical cavity containing liquid |
| $\hat{H}$ | $(\rho S \ell/2m)\,(V/\ell)\left[C_{N_\alpha} - k_y^{-2}\left(C_{M_q} + C_{M_{\dot{\alpha}}}\right)\right]$ |

| | |
|---|---|
| $h$ | distance from the gyroscope's pivot location to the center of the cylindrical cavity |
| $I_x$, $I_y$ | axial and transverse moments of inertia of the gyroscope or projectile |
| $K_j$ | magnitude of the j-th yaw arm (j=1, 2) |
| $K_{jo}$ | initial value of $K_j$ |
| $k_x$ | $(I_x/m\ell^2)^{1/2}$, the projectile's axial radius of gyration |
| $k_y$ | $(I_y/m\ell^2)^{1/2}$, the projectile's transverse radius of gyration |
| $\ell$ | reference length |
| $\hat{M}$ | $(\rho S\ell^3/2I_y)\ (V/\ell)^2\ C_{M_\alpha}$ |
| $M_L\tilde{Y}$, $M_L\tilde{Z}$ | components of the aerodynamic moment |
| $m$ | projectile mass |
| $m_L$ | liquid mass in a fully filled cylindrical cavity |
| Re | $a^2\dot{\phi}/\nu$, Reynolds number |
| $S$ | reference area |
| $s_g$ | $\sigma^2\dot{\phi}^2/4\hat{M}$, the gyroscope stability factor |
| $\hat{T}$ | $(\rho S\ell/2m)\ (V/\ell)\left[C_{N_\alpha} + k_x^{-2}\ C_{M_{p_\alpha}}\right]$ |
| $t$ | time |
| $V$ | magnitude of the projectile's velocity vector |
| $\varepsilon$ | nondimensionalized growth rate for single mode motion, j=1 |

| | |
|---|---|
| $\varepsilon_j$ | nondimensionalized growth rate of the j-th yaw mode (j=1, 2) |
| $\nu$ | kinematic viscosity |
| $\tilde{\xi}$ | complex yaw in the nonrolling coordinate system |
| $\rho$ | air density |
| $\sigma$ | $I_x/I_y$ |
| $\tau$ | $\tau_j$ for one-mode yawing motion |
| $\tau_j$ | $\dot{\phi}_j/\dot{\phi}$, the nondimensionalized frequency of the j-th yaw mode (j=1, 2) |
| $\phi$ | $\dot{\phi}\, t$ |
| $\phi_j$ | $\phi_{jo} + \tau_j \dot{\phi}\, t$ (j=1, 2) |
| $\phi_{jo}$ | initial orientation angle of the j-th yaw arm (j=1, 2) |
| $\dot{\phi}$ | spin rate (assumed to be positive) |

Superscripts

| | |
|---|---|
| $(\rightarrow)$ | vector quantity |
| $(\cdot)$ | time derivative |

DISTRIBUTION LIST

| No. of Copies | Organization |
|---|---|
| 12 | Administrator<br>Defense Technical<br>Information Center<br>ATTN: DTIC-DDA<br>Cameron Station<br>Alexandria, VA 22314 |
| 1 | Commander<br>US Army Materiel Development<br>and Readiness Command<br>ATTN: DRCDMD-ST<br>5001 Eisenhower Avenue<br>Alexandria, VA 22333 |
| 1 | Commander<br>US Army Armament Research<br>and Development Command<br>ATTN: DRDAR-TDC, Dr. D. Gvorog<br>Dover, NJ 07801 |
| 2 | Commander<br>US Army Armament Research<br>and Development Command<br>ATTN: DRDAR-TSS<br>Dover, NJ 07801 |
| 1 | Commander<br>US Army Armament Research<br>and Development Command<br>ATTN: DRDAR-LC<br>Dr. J. T. Frasier<br>Dover, NJ 07801 |
| 1 | Commander<br>US Army Armament Research<br>and Development Command<br>ATTN: DRDAR-CAWS-AM<br>Mr. DellaTerga<br>Dover, NJ 07801 |
| 2 | Commander<br>US Army Armament Research<br>and Development Command<br>ATTN: DRDAR-LCA-F<br>Mr. D. Mertz<br>Mr. A. Loeb<br>Dover, NJ 07801 |

| No. of Copies | Organization |
|---|---|
| 1 | Commander<br>US Army Armament Materiel<br>Readiness Command<br>ATTN: DRSAR-LEP-L<br>Rock Island, IL 61299 |
| 1 | Director<br>US Army Armament Research<br>and Development Command<br>Benet Weapons Laboratory<br>ATTN: DRDAR-LCB-TL<br>Watervliet, NY 12189 |
| 1 | Commander<br>US Army Aviation Research<br>and Development Command<br>ATTN: DRDAV-E<br>4300 Goodfellow Blvd<br>St. Louis, MO 63120 |
| 1 | Director<br>US Army Air Mobility Research<br>and Development Laboratory<br>Ames Research Center<br>Moffett Field, CA 94035 |
| 1 | Commander<br>US Army Communications Research<br>and Development Command<br>ATTN: DRSEL-ATDD<br>Fort Monmouth, NJ 07703 |
| 1 | Commander<br>US Army Electronics Research<br>and Development Command<br>Technical Support Activity<br>ATTN: DELSD-L<br>Fort Monmouth, NJ 07703 |
| 1 | Commander<br>US Army Missile Command<br>ATTN: DRSMI-R<br>Redstone Arsenal, AL 35898 |
| 1 | Commander<br>US Army Missile Command<br>ATTN: DRSMI-YDL<br>Redstone Arsenal, AL 35898 |

DISTRIBUTION LIST

| No. of Copies | Organization |
|---|---|
| 1 | Commander<br>US Army Tank Automotive Command<br>ATTN: DRSTA-TSL<br>Warren, MI 48090 |
| 1 | Director<br>US Army TRADOC Systems Analysis Activity<br>ATTN: ATAA-SL<br>White Sands Missile Range<br>NM 88002 |
| 1 | Director<br>US Army Dugway Proving Ground<br>ATTN: STEDP-MT<br>Mr. G. C. Travers<br>Dugway, UT 84022 |
| 1 | Commander<br>US Army Yuma Proving Ground<br>ATTN: STEYP-MTW<br>Major S. Thorlin<br>Yuma, AZ 85365 |
| 1 | Commandant<br>US Army Field Artillery School<br>ATTN: ATSF-CD-MW (LT Bryan)<br>Ft. Sill, OK 73503 |
| 1 | President<br>US Army Field Artillery School<br>ATTN: ATZR-BD-WT (CPT Dawson)<br>Ft. Sill, OK 73503 |
| 2 | Director<br>Sandia Laboratories<br>ATTN: Mr. H. R. Vaughn<br>Dr. W. Oberkampf<br>Albuquerque, NM 87115 |
| 2 | Commandant<br>US Army Infantry School<br>ATTN: ATSH-CD-CSO-OR<br>Fort Benning, GA 31905 |
| 1 | Stanford University<br>Department of Aeronautics and Astronautics<br>ATTN: Dr. Sukumar Chakravarthy<br>Stanford CA 94305 |
| 1 | The University of Rochester<br>Department of Mechanical and Aerospace Sciences<br>ATTN: Dr. Roger F. Gans<br>Rochester, NY 14627 |

Aberdeen Proving Ground

Director, USAMSAA
ATTN: DRXSY-D
DRXSY-MP, Mr. H. Cohen

Commander, USATECOM
Bldg. 314, AA
ATTN: DRSTE-TO-F
DRSTE-CM-F
Mr. Gibson (2 cys)

PM-SMOKE, Bldg. 324, AA
ATTN: DRCPM-SMK-M (MAJ Gober)

Director, USACSL
Bldg. E3330, EA
ATTN: DRDAR-CLN
Mr. W. Dee
Mr. McKivrigan
Mr. F. Dagostin
Mr. C. Hughes

Director, USACSL
Bldg. E3516, EA
ATTN: DRDAR-CLB-PA
Mr. M. Miller
DRDAR-CLB-PA
DRDAR-CLN
DRDAR-CLJ-L

## USER EVALUATION OF REPORT

Please take a few minutes to answer the questions below; tear out this sheet, fold as indicated, staple or tape closed, and place in the mail. Your comments will provide us with information for improving future reports.

1. BRL Report Number _____

2. Does this report satisfy a need? (Comment on purpose, related project, or other area of interest for which report will be used.)

_____

_____

_____

3. How, specifically, is the report being used? (Information source, design data or procedure, management procedure, source of ideas, etc.) _____

_____

_____

4. Has the information in this report led to any quantitative savings as far as man-hours/contract dollars saved, operating costs avoided, efficiencies achieved, etc.? If so, please elaborate.

_____

_____

5. General Comments (Indicate what you think should be changed to make this report and future reports of this type more responsive to your needs, more usable, improve readability, etc.) _____

_____

_____

_____

6. If you would like to be contacted by the personnel who prepared this report to raise specific questions or discuss the topic, please fill in the following information.

Name: _____

Telephone Number: _____

Organization Address: _____

_____

_____